Copyright Warning & Restrictions

The copyright law of the United States (Title 17, United States Code) governs the making of photocopies or other reproductions of copyrighted material.

Under certain conditions specified in the law, libraries and archives are authorized to furnish a photocopy or other reproduction. One of these specified conditions is that the photocopy or reproduction is not to be "used for any purpose other than private study, scholarship, or research." If a, user makes a request for, or later uses, a photocopy or reproduction for purposes in excess of "fair use" that user may be liable for copyright infringement,

This institution reserves the right to refuse to accept a copying order if, in its judgment, fulfillment of the order would involve violation of copyright law.

Please Note: The author retains the copyright while the New Jersey Institute of Technology reserves the right to distribute this thesis or dissertation

Printing note: If you do not wish to print this page, then select "Pages from: first page # to: last page #" on the print dialog screen

NJIT New Jersey's Science & Technology University

The Van Houten library has removed some of the personal information and all signatures from the approval page and biographical sketches of theses and dissertations in order to protect the identity of NJIT graduates and faculty.

FLOW TUBE REACTIONS OF SELECTED CHLOROCARBONS WITH MOLECULAR HYDROGEN OR WATER VAPOR IN A MICROWAVE INDUCED PLASMA REACTOR

by

Robert Benedict Barat

Thesis submitted to the Faculty of the Graduate School of the New Jersey Institute of Technology in partial fulfillment of the requirements of Master of Science in Chemical Engineering

1983

APPROVAL SHEET

Title of Thesis: FLOW TUBE REACTIONS OF SELECTED CHLOROCARBONS WITH MOLECULAR HYDROGEN OR WATER VAPOR IN A MICROWAVE INDUCED PLASMA REACTOR

Name of Candidate: Robert Benedict Barat
Master of Science in Chemical Engineering, 1983

Thesis and Abstract Approved:

Dr. Joseph W. Bozzelli — date 5/10/83
Associate Professor
Dept. of Chemical
Engineering and Chemistry

Signatures of Remaining Members of Thesis Committee:

Dr. Barbra Kebbekus — date 5/10/83

Dr. Gordon Lewandowski — date 5/10/83

VITA

Name: Robert Benedict Barat

Permanent address:

Degree and date to be conferred: M. Sc. in ChE., 1983

Date of birth:

Place of birth:

Secondary education: Roselle Catholic, Roselle, N.J.

Collegiate insts. attended	Dates	Degree	Date of Degree
New Jersey Institute of Technology	9/76-5/80	B.S.	May 1980
New Jersey Institute of Technology	9/80-5/83	M.S.	May 1983

Major: Chemical Engineering

Publications: R. B. Barat and J. W. Bozzelli, "Variable Power Microwave Discharge and Cavity," Review of Scientific Instruments, 52(4), 612 (1981).

Positions held:

a) Research assistant, Dept. of Chemical Engineering and Chemistry, New Jersey Institute of Technology, Newark, N.J. 07102 Jan. 1983 - Aug. 1983.

b) Project engineer, Exxon Research and Engineering Company, Florham Park, N.J. 07932 June 1980 - Dec. 1982.

ABSTRACT

Title of Thesis: FLOW TUBE REACTIONS OF SELECTED CHLOROCARBONS WITH MOLECULAR HYDROGEN OR WATER VAPOR IN A MICROWAVE INDUCED PLASMA REACTOR

Robert B. Barat, Master of Science in Chemical Engineering, 1983

Thesis directed by: Dr. Joseph W. Bozzelli, Associate Professor

The reactions of various chlorinated hydrocarbons with molecular hydrogen or water vapor have been studied in a microwave plasma tubular flow reactor. The investigation of such reactions is desireable because the often toxic parent chlorocarbons are transformed to more thermodynamically stable and relatively non-toxic products by removal of chlorine atoms as hydrogen chloride. Present detoxification technologies generally employ thermal oxidation as a means of disposal of chlorocarbons, which does not offer a thermodynamically stable sink for the chlorine atoms.

The experimental apparatus included feed introduction systems, a microwave plasma reactor, and full product analyses. The feed systems enabled use of gases and vapors

from both relatively volatile and non-volatile liquids. The microwave plasma offers an interesting and unusual approach to chemical reactions. Because of the reactivity of such a discharge system, reactions are achieved to significant conversion levels without the high temperatures required in a conventional thermal reactor. Full product analyses were performed with flame ionization and thermal conductivity gas chromatography, mass spectrometry, and pH detection for HCl.

The reaction systems studied were chloroform / molecular hydrogen, trichloroethylene / molecular hydrogen, trichloroethylene / water vapor, and mono-chlorobenzene / molecular hydrogen. Ranges of conversions of the parent chlorocarbons were achieved, in some cases as wide as 50 to nearly 100 percent. Product analysis indicates conversions to hydrogen chloride, light hydrocarbons, and non-parent chlorocarbons when molecular hydrogen is used. Use of water vapor as a hydrogen source yields similar results, except that carbon monoxide replaces many of the light hydrocarbons. With either molecular hydrogen or water vapor present, at least 85 mole percent of the chlorine atoms in the converted parent chlorocarbons form thermodynamically stable hydrogen chloride for parent conversions of 80 percent or more. The remaining chlorine atoms in the converted parent were present as non-parent chlorocarbons.

Water vapor was more effective than molecular hydrogen in decomposing trichloroethylene. The amount of water vapor required for a given conversion was an order of magnitude smaller than the required hydrogen. The overall rate

constant for the water reaction was about double that for hydrogen at comparable electric input power levels. When their relative cost is also considered, water vapor would appear to be much more desireable for a commercial process.

In addition to full product analysis, preliminary kinetic analyses were performed with reaction mechanisms postulated. The reactions in the plasma were found to follow one-half order kinetic dependence on each of the feed reagents. The plasma reactor exhibited reactivity which varied in an Arrhenius fashion with input electrical power to the microwave generator.

DEDICATION

This thesis is hereby dedicated to the pursuit of higher learning, the quest for the knowledge which enables one to lead a scientific and engineering career, making independent choices, totally in control of one's destiny.

ACKNOWLEDGEMENT

I hereby acknowledge the tremendous assistance of my advisor, Dr. Joseph W. Bozzelli, who has strived to teach me to think, not only as an engineer, but also as a scientist.

TABLE OF CONTENTS

Chapter Page

Dedication....ii

Acknowledgement....iii

List of Tables....iv

List of Figures....v

I. INTRODUCTION....1

1. Oxidation / Reduction of Halocarbons....2

2. The Microwave Plasma Reactor....8

3. Uses of Plasmas....15

II. EXPERIMENTAL APPARATUS AND PROCEDURE....17

III. RESULTS AND DISCUSSION....27

1. Reactor Analysis....27

2. $CHCl_3$ / H_2....30

3. C_2HCl_3 / H_2....44

4. C_2HCL_3 / H_2O....55

5. C_6H_5Cl / H_2....69

6. An Arrhenius Form of the Kinetic Rate Constants....73

IV. CONCLUSIONS....78

V. APPENDIX....82

1. $CHCl_3$ + H_2 Mechanism....82

2. $CHCl_3$ + H_2 Alternate Mechanism....84

3. C_2HCl_3 + H_2 Mechanism.....91

3a. C_2HCl_3 + H_2 Parallel Mechanism.....93

4. C_2HCl_3 + H_2 Alternate Mechanism.....95

5. C_2HCl_3 + H_2O Mechanism.....99

6. Calculation of Initial Chlorocarbon Concentration C_{Ao} and Feed Rate F_{Ao}.....101

7a. Data for Kinetic Analysis.....105

7b. Cumulative Product Distributions.....108

7c. Data for Arrhenius-type Experiment.....111

VI. REFERENCES.....112

LIST OF TABLES

Table page

1. Selected Bond Strengths.....3

2. Thermodynamic Equilibria of Selected Reactions.....6

3. Sample Product Distribution $CHCl_3 + H_2$.....31

4. Sample Product Distribution $C_2HCl_3 + H_2$.....45

5. Sample Product Distribution $C_2HCl_3 + H_2O$.....56

6. Sample Product Distribution $C_6H_5Cl + H_2$.....71

LIST OF FIGURES

Table page

1. Variation of Electric Field Strength with Time.....11
2. System Block Diagram.....18
3. Liquid Chlorocarbon Impinger Feed System.....20
4. Heated Reservoir Feed System.....21
5. Plasma Reactor and Waveguide.....22
6. Sample Collection System for GC/FID.....24
7. Carbon Balance for $CHCl_3 + H_2$.....32
8. Chlorine Balance for $CHCl_3 + H_2$.....34
9. Kinetic Plot for $CHCl_3 + H_2$.....37
10. Carbon Balance for $C_2HCl_3 + H_2$.....46
11. Chlorine Balance for $C_2HCl_3 + H_2$.....47
12. Kinetic Plot for $C_2HCl_3 + H_2$.....49
13. Carbon Balance for $C_2HCl_3 + H_2O$.....57
14. Chlorine Balance for $C_2HCl_3 + H_2O$.....59
15. Kinetic Plot for $C_2HCl_3 + H_2O$.....62
16. Carbon Balance for $C_6H_5Cl + H_2$.....70
17. Variation in Rate Constant with Electric Power Input for $CHCl_3 + H_2$.....76

1. INTRODUCTION

1. Oxidation / Reduction of Halocarbons

The disposal of hazardous wastes has recently become a major environmental as well as political issue in the United States. Incidents such as Love Canal in Niagra, New York and Chemical Control in Elizabeth, New Jersey point to the severity of the problem. Many of the hazardous waste species are chlorinated hydrocarbons used as solvents, pesticides, and heat transfer fluids. Examples include polychlorinated biphenyls (PCB), dichlorodiphenyltrichlorethane (DDT), and carbon tetrachloride. In the past, random burial was the accepted disposal method. More acceptable disposal options such as reclamation, detoxification by chemical reaction, and supervised burial are now under development and in progress.

Many recent research efforts on chemical detoxification of chlorinated wastes have concentrated on oxidation as a means to convert carbon species to carbon dioxide (CO_2). High temperature incineration is presently considered a practical first generation technology in chemical detoxification. Present design criteria as established by the Federal Environmental Protection Administration (EPA) requires combustion temperatures of 2000 ^{o}F and a two second residence time in order to achieve the greater than 99.99% destruction of the parent compound (1). One method being tested adds liquid chlorinated wastes to petroleum fuel oil to be combusted in excess air in a cement kiln (2). Other

oxidation approaches under study convert parent halocarbons such as CCl_4, DDT, and PCB to CO_2 and other carbon - chlorine adducts. Roberts and Sawyer (3) have employed dimethyl sulfoxide and dimethylformamide solutions of super oxide ion to convert CCl_4 to solutions of carbonates and chlorides. Pytlewski, et. al. (4) have suspended neutral sodium in solutions of polyethylene glycol to convert PCB. Botre, et. al. (5) used surfactant solutions of chloriodides to degrade dioxins. Catalytic oxidation of halocarbon species in complex molten salt reactors has been studied by several investigators. Hertzler, et. al. (6) oxidized selected chlorocarbon species in a microwave plasma vapor phase tubular flow reactor. While achieving the required 99.99+% destruction of the parent compound, no analysis was made of total reactor effluent in the above studies. Two industrial processes include the Zimpro - wet air oxidation (7) and the IT - Enviroscience oxidation by NO_3^- in a solution of CH_2O. These processes, however, are not effective for chlorinated hydrocarbons. One interesting suitable method under study reacts halocarbons with supercritical water (8).

Despite the present recommendation of oxidation as the preferred method for destruction of halogenated hydrocarbons, such processes do not provide for a thermodynamically favorable sink for the halogen atoms. While the carbon atoms convert to CO_2, a consideration of bond strengths (see Table 1) shows that the C-Cl bond is the most thermodynamically favorable sink for the chlorine atoms in the oxygen environment. In fact, chlorinated and brominated hydrocarbons form

TABLE 1

SELECTED BOND STRENGTHS*

(kcal/mole at 298 K)

BOND	STRENGTHS
C-C	140
C=C	170
C≡C	230
H-Cl	103
C-Cl	75-81
C-H	80-113
H-H	104
H-OH	119
H-O	102
C=O	257
O=CO	128
O=O	119
O-Cl	64
Cl-N	62
Cl-Cl	58

* Ref. (28)

the basis for many fire retardents. The use of chlorinated wastes as a fuel "supplement" in a kiln operation requires low waste concentrations for proper flame maintenance.

Reactions of Cl containing species in an oxidizing atmosphere can lead to Cl containing byproducts such as phosgene, chlorinated aldehydes and acids, and smaller chlorinated hydrocarbons. Arnold, et. al. (9) characterized the emission spectra from flames produced in the reaction of atomic oxygen with selected chlorocarbons. For the reaction of O and $CHCl_3$, Arnold found CCl_4, CCl_2O, Cl_2, HCl, CO_2, and CO. He observed C_2H_2, CH_4, Cl_2, HCl, CO, and CO_2 products from the reaction of O with CH_2Cl_2. The production of hexachlorobenzene (C_6Cl_6) from oxidation of pentachlorophenol (C_6Cl_5OH) is thermodynamically favorable and has been observed (10). Rubey and Duvall thermally decomposed PCB in a flow reactor and observed C_6Cl_6 and smaller chlorine containing species (11). These observations all indicate the relative thermodynamic stability of the C-Cl bond in the presence of oxygen and the absence of hydrogen. While some of these methods may meet EPA destruction requirements, an analysis of the potential toxicity of reaction byproducts has received little emphasis to date. It is the substituent Cl atoms that often are responsible for the toxicity of these compounds, and oxidation does not offer a thermodynamically favorable sink for the Cl atoms. The result may often be byproducts with properties as undesireable as the parent compound.

The use of the hydrogen atom as a thermodynamically

favorable sink for Cl atoms results in the Cl being removed as HCl (see Table 1). From a gas phase reaction system, HCl can be scrubbed out with water or a caustic solution and effectively neutralized. The H-Cl bond (103 kcal/mole) is significantly favored over the C-Cl bond (81 kcal/mole). The favored thermodynamics of the reactions of halocarbons with hydrogen or water, also a source of hydrogen, is evident from the large equilibrium constants (K_p) listed in Table 2. In work similar to that of Arnold, Chari (12), reacted externally generated H atoms with C_1 and C_2 halocarbons and observed HCl and CH emission in the infrared and ultraviolet - visible regions respectively. Mass spectral analysis showed the reaction products to be HCl, low molecular weight hydrocarbons, and some lighter chlorinated species. Westenberg and deHaas (13) have measured rate constants for the reactions of H atoms with selected halogenated methanes in a fast flow reactor. For the relativley fast reaction of CF_3Br with H, a room temperature rate constant was found to be 1.03×10^{10} sec^{-1} $mole^{-1}$ cm^3. Costes, et. al. (14) have also studied the reations of atomic hydrogen with CCl_4 in a low pressure reactor, showing the production of atomic carbon. Reactions of chlorinated solvents with hydrogen in a tubular flow reactor at elevated temperatures (500+ ^{o}C) by Chuang (15) have shown high conversion of the reagent to HCl and lower hydrocarbons, along with solid graphitic carbon deposits. Early studies (16) of the reactions of chlorinated solvents in a high temperature tubular flow reactor substituting water as a hydrogen source have shown high conversion

TABLE 2

THERMODYNAMIC EQUILIBRIA OF SELECTED REACTIONS*

$CCl_4 + 4\ H_2 = 4\ HCl + CH_4$

T (K)	K_p
300	3.2×10^{65}
800	6.1×10^{26}

$CCl_4 + 2\ H_2O = 4\ HCl + CO_2$

T (K)	K_p
300	3.8×10^{43}
800	7.6×10^{25}

$C_6Cl_6 + 15\ H_2 = 6\ CH_4 + 6\ HCl$

T (K)	K_p
300	Infinity
800	8.4×10^{50}

$C_6Cl_6 + 12\ H_2O = 6\ CO_2 + 6\ HCl + 9\ H_2$

T (K)	K_p
300	7.1×10^{41}
800	1.0×10^{45}

* Ref. (28)

of the parent reagent to HCl, lower hydrocarbons, and carbon oxides, with some graphitic carbon byproduct. It is clear, then, that reaction of halogenated species with hydrogen introduced either as H, H_2, or as H_2O offers a viable means of detoxification through halogen removal as hydrogen halide.

2. The Microwave Plasma Reactor

An interesting approach to the reactions of halocarbons with other species is the application of a plasma discharge. As previously mentioned, Hertzler, etal (6) oxidized halocarbons with molecular oxygen directly in a low pressure tubular flow microwave plasma discharge reactor. While excess O_2 was utilized and the required 99.99+% destruction of parent compound was obtained, there was, however, no full product analysis. Subsequent determination of the toxicity of products was therefore unknown. Chari (12), Westenberg and deHaas (13), and Costes (14), generated atomic hydrogen in separate discharges, then reacted these atoms with halocarbons in reactors well downstream of the plasma zone. The present study combines the interesting features of a plasma discharge as both a free radical generator and reactor with the thermodynamic desireability of reacting halocarbons in the presence of hydrogen in a single fast flow system. Halocarbons are reacted with molecular hydrogen or water vapor in a fast flow tubular reactor in which a microwave plasma discharge is maintained.

The decision to use a plasma discharge reactor in the present study came about as a result of two factors. First, the work by Chuang (15) with a tubular flow thermal reactor showed significant residual solid carbon formation in the reactions of chlorocarbons and molecular hydrogen. This had been attributed to pyrolysis at the elevated temperatures required for complete reaction (above 700 ^{o}C) in the thermal

reactor. The plasma reactor operates at much lower gas temperatures (est. below 200 ^{o}C) while employing kinetically energetic free electrons to initiate the reactions. It was felt that the residual carbon buildup could be eliminated or reduced by the lower reactor gas temperatures as well as the lower pressures (under 20 Torr as compared to 1-2 atm for the thermal reactor) characteristic of the plasma reactor. Second, earlier studies (12), (13), (14) reported on the reaction of externally generated atomic hydrogen and halocarbons leading to flames, atomic carbon production, and eventual halocarbon conversion to the hydrogen halide and methane through chain branching mechanisms. Our choice of a plasma reactor generates atomic hydrogen in the plasma (i.e. in situ) in the same region as the halocarbon conversion reactions are to occur. This offers the opportunity of a greater density of the atomic hydrogen required for halocarbon conversion in addition to free electron impact upon the chlorocarbon reagent molecules themselves. Atomic species separately generated in one reactor and then transported to another reactor zone for kinetic studies with stable species are subject to depletion mechanisms of recombination catalyzed by carrier gas molecules and the flow tube walls.

A plasma is a state of matter characterized as a complex and dynamic gas phase system of free radicals, molecules, ions, atoms, free electrons, and excited species. Plasmas can be sustained with very high temperatures (> 2000 K) or strong electric, magnetic, or electromagnetic fields. For

example, an activated florescent light contains a plasma initiated by a voltage discharge across two internal electrodes and sustained by an oscillating (60 Hz) electric field. In the present study, microwave electromagnetic radiation initiates and sustains the plasma inside a flow tube which acts as the reactor.

The microwave plasma in this study is initiated by the interaction of free electrons in the gas (initially, naturally occuring or generated with a high voltage Tesla Coil and subsequently self sustaining) with electromagnetic microwave radiation oscillating in a resonant cavity at a frequency of 2.45×10^9 cycles /second (2.45 Giga Hz). The electrons are accelerated by the oscillating electric field of the microwave and attain a high degree of kinetic energy. A typical electromagnetic wave is shown in Figure 1. The electron acceleration can be represented as

$$e^- + E/M \text{ ----> } e^- (KE) \qquad (1)$$

where e^- is an electron, e^- (KE) is an electron with high translational kinetic energy, and E/M is an electromagnetic wave. The high kinetic energy electron now initiates reactions of the reagent species fed directly to the plasma by collision and energy transfer with stable reactants or metastable intermediates in the plasma, producing additional reactive species as shown in the following equations:

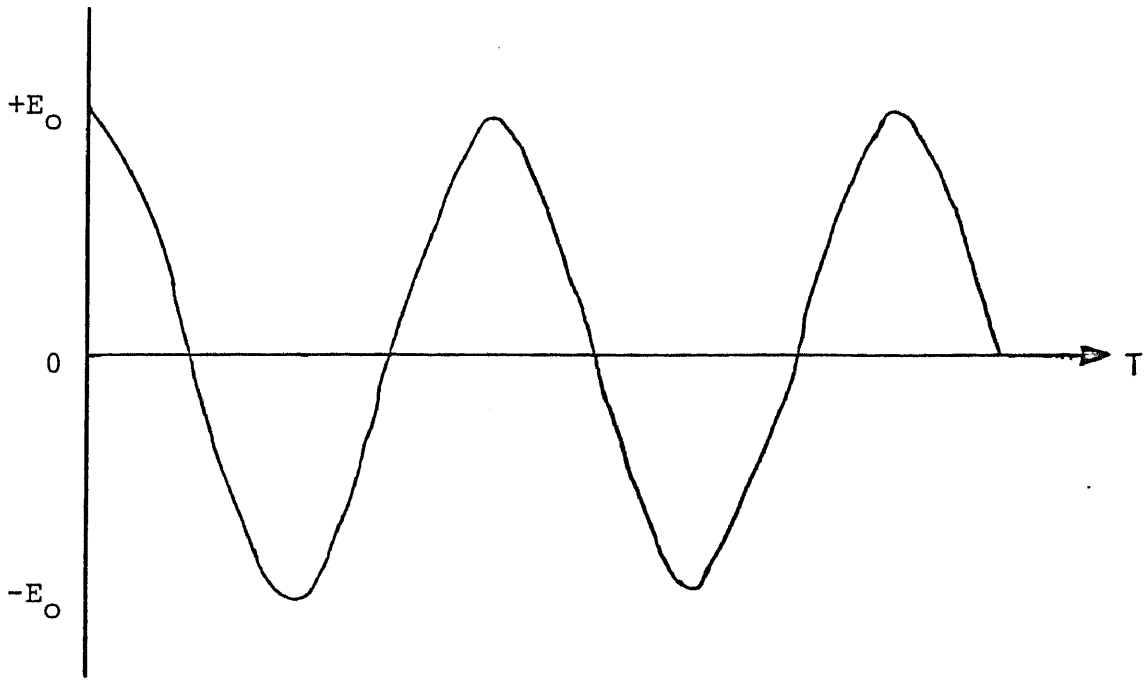

$$E = E_0 \sin (2\pi \nu T)$$

VARIATION OF ELECTRIC FIELD STRENGTH WITH TIME

AT A FIXED POSITION

MICROWAVE FREQUENCY $\nu = 2.45 \times 10^9$ SEC^{-1}

WAVELENGTH $\lambda = c/\nu = 12$ CM

FIGURE 1

$$e^- (KE) + A \text{ -----> } A^* + e^- \quad (2)$$

$$e^- (KE) + A \text{ -----> } A^+ + 2e^- \quad (3)$$

$$A^* \text{ -----> } a + b \quad (4)$$

$$e^- (KE) + AB \text{ -----> } A^+ + B + 2e^- \quad (5)$$

$$a + C \text{ -----> other reactions/species} \quad (6)$$

Species A, AB, and C are neutral molecules; a , b , and B are free radicals; A^+ is and ion; and A^* is an excited species. Within a short period of time (several micro-seconds), a steady state is achieved in the plasma reaction zone between various initiation, transfer, branching and termination reactions.

The microwave discharge is an example of or also designated as a "glow discharge" due to the emission of visible as well as other radiation from excited species in the plasma. The kinetically energetic free electrons within the glow discharge have average energies of 1 to over 10 electron volts (ev) and densities of 10^9 to 10^{12} / cm^3 (17). An electron temperature T_e can be assigned which characterizes the average electron translational energy. A gas temperature T_g can also be assigned. This is the traditional measure of average thermal energy of gas molecules which one would obtain with a conventional thermocouple mearsurement. In the plasma, the ratio of T_e to T_g is in the range of 10 to 100 (17). This means that the plasma has neutral species with energies corresponding to near ambient gas temperatures, but has highly energetic free electrons which can rupture molecular bonds (17) and/or create species in highly excited

electronic, vibrational, and rotational states. This is the fundamental difference between a thermal or conventional catalytic gas phase reactor and a plasma reactor. In a thermal system, gas temperature is the handle on average molecular energies and bond breaking and product formation. In catalytic systems, catalyst activity is the key to reactivity. In a plasma reactor, collision with high energy free electrons and free radicals and excited species, which are at relatively high steady state levels, are key to initiating reactions and formation of products.

This distinction between thermal (i.e. gas temperature) energy and electron (i.e. electron temperature) energy is evident in the work of Brown and Bell (18) on the kinetics of carbon monoxide oxidation and carbon dioxide decomposition. Using a radio frequency (13.56 Mega Hz) generator to sustain a plasma in a tubular flow reactor, the oxidation of CO to CO_2 and the decomposition of CO_2 to CO and O_2 were studied as a function of discharge power input, reactor pressure, and feed flow rates. Analysis showed that the composition of plasma reactor effluent is uniquely determined at high powers and is independent of whether the feed consisted of CO_2 only or stoichiometric amounts of CO and O_2. In addition, at a given pressure and power input, the product composition is independent of flow rate below a certain feed rate. Brown and Bell concluded that these states were "kinetic steady states" wherein space time was sufficiently long for achievement of what appeared to be a chemical reaction equilibrium. However, thermal reaction equilibrium temperatures (i.e. gas

temperatures) calculated using product compositions were significantly higher than thermocouple measured gas temperatures in the plasma. They further concluded that this "kinetic steady state" corresponded to a balance between forward and reverse reactions within the space time of the reactor which could not be described by traditional thermal reaction equilibrium. They attributed the discrepancy to electron impact reactions which are major sources of the atomic intermediates in the plasma through which reactants are converted to products. Inclusion of these impact reactions characterized by electron temperatures T_e in a mechanism of molecular and free radical reactions described by gas temperatures T_g produced a predictive model yielding good correspondence to the experimental data, including description of the "kinetic steady states".

3. Uses of Plasmas

There are numerous applications of plasmas, only one of which is destruction of toxic chemicals (6), (19). The widespread use of plasmas has been facilitatesd by the development of electronics and receiving and transmitting antennas necessary to maintain plasmas over pressure ranges from several atmospheres down to below 1 Torr. Radio frequency (RF) inductively coupled argon plasmas (ICAP) are extensively used in the generation of excited atoms which emit photons of a specific wavelength for trace level multi-element analysis by atomic emission spectroscopy (20). Electric direct current (DC) plasma discharges have also been routinely used for atomic species generation and as light sources (9), (12), (13), (14), (21), (22). Microwave discharges have been used for the generation of atomic and free radical species (23), laser initiation (24), and spectroscopic light sources (25).

An interesting and rapidly growing plasma application is etching of semiconductor surfaces for integrated circuit (IC) manufacture. Gottscho, et. al. (26) are studying radio frequency CCl_4 plasmas as a means of etching surfaces such as GaAs and InP. A desireable characteristic of plasma etching over wet chemistry methods is its reproducibility. One undesireable trait is some residual surface contamination by carbonaceous material for carbon containing feeds. This area offers a promising future for plasmas.

Reviews of plasma techniques and applications can be

found in Baddour and Timmins (27) and Hollahan and Bell (17).

II. EXPERIMENTAL APPARATUS AND PROCEDURE

The experimental apparatus used in this study consists of a feed vapor generation, metering, and delivery manifold system; a quartz tubular plug flow reactor; a microwave power generator with waveguide; and several reactor effluent sampling systems. The sampling systems include flame ionization and thermal conductivity gas chromatography (GC/FID) and (GC/TCD), GC/Mass spectrometry (GC/MS), and specific ion or pH measurements. Grab samples are taken for separate analysis by GC/MS while the GC/FID, GC/TCD, and pH analytical capabilities are on-line. A block diagram of the entire system is shown in Figure 2.

The reagent inlet metering and delivery systems are designed to permit input of gas or vapor to the reactor flow tube at pressures between 0.5 and 10 mm Hg. A liquid impinger system is used for those cases where the reactants include a non-condensable gas (at ambient conditions) and a relatively volatile liquid . For cases involving relatively non-volatile liquid reactants, heated liquid reservoirs are used as vapor generators. Finally, non-condensable gases can be fed to the flow system directly through needle valves and rotameters.

In the first system, hydrogen gas is passed through a rotameter and then bubbled through two impingers (in series) operating at 1.5 psig. The impingers are filled with the liquid halocarbon reagent so the H_2 becomes saturated with the halocarbon vapor. The gas mixture then flows to the

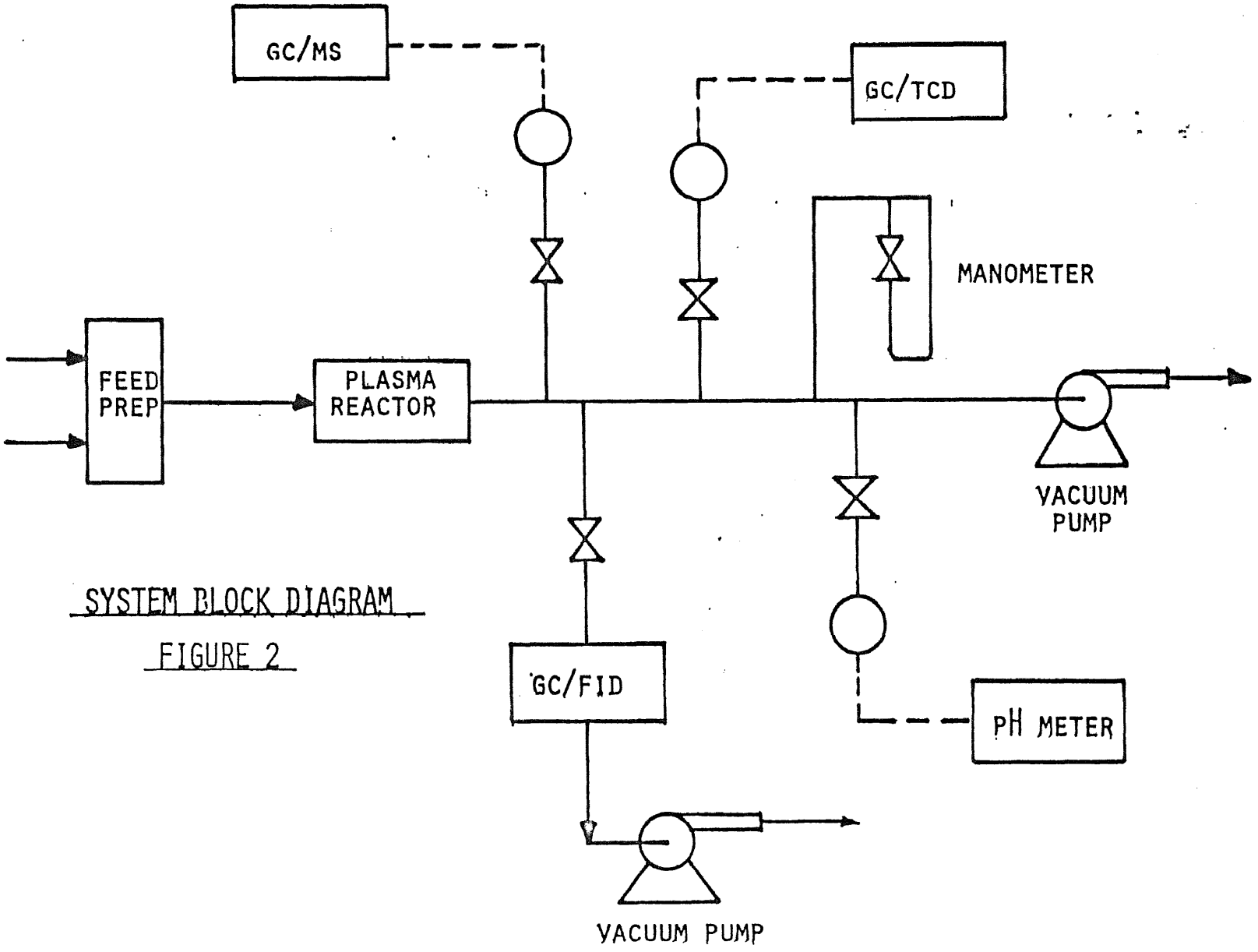

SYSTEM BLOCK DIAGRAM

FIGURE 2

inlet manifold of the quartz reactor where it mixes with an additional stream of pure H2. The total mixture flows from the manifold into the reactor. A block diagram of this inlet metering and delivery system is shown in Figure 3.

In the second feed system, vapor is generated in heated liquid reservoirs. Proportional temperature controllers maintain vapor pressures in the vapor space of the reservoir at approximately one atmosphere (100 kPa) absolute. Vapor is throttled across a needle valve and fed to the flow system. An off-line manometer and evacuated volume system is used to meter the vapor at reduced pressures to prevent condensation. For a measurement, vapor is redirected to the metering system where it fills a known volume to a measured pressure and time duration. This system is shown in Figure 4.

The reactions between H_2 or H_2O vapor and the halocarbons occur in a 2.15 cm ID quartz plug flow reactor within which a stable plasma is established and maintained. The flow tube passes through a waveguide in which a resonant wave pattern of microwave radiation is maintained. The tube passes through at a 130 degree angle to ensure efficient coupling of the microwave radiation into the flowing gas, thereby inducing and maintaining a plasma without the need for internal electrodes. The waveguide and reactor tube are cooled with small electronic fans (50 lps) and compressed air. The reactor and waveguide are shown in Figure 5.

The microwave power originates from a 0.6 kilowatt (kW) Mitsubisi magnetron and power supply which were original components in a conventional microwave oven. The waveguide

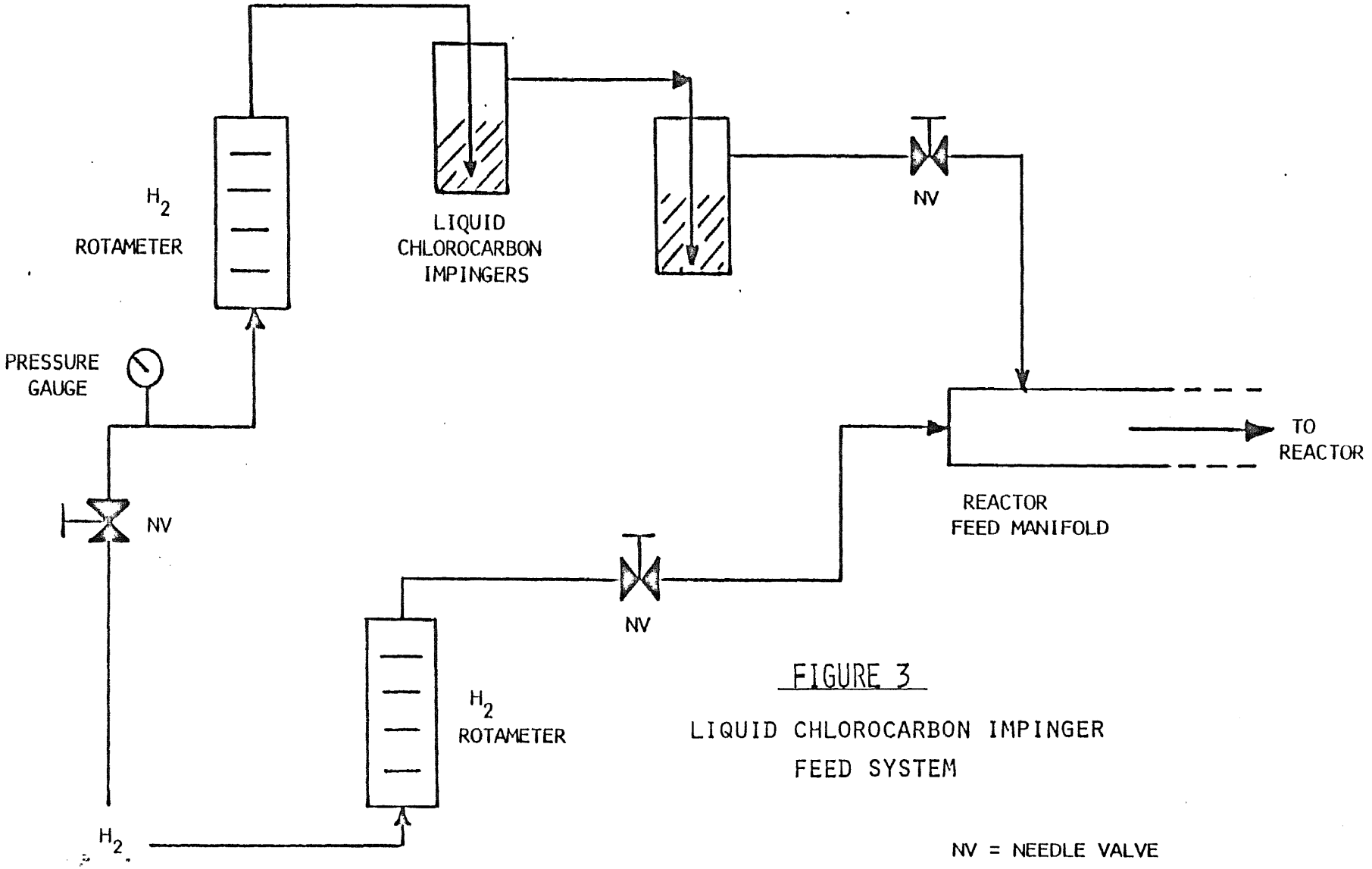

FIGURE 3

LIQUID CHLOROCARBON IMPINGER
FEED SYSTEM

NV = NEEDLE VALVE

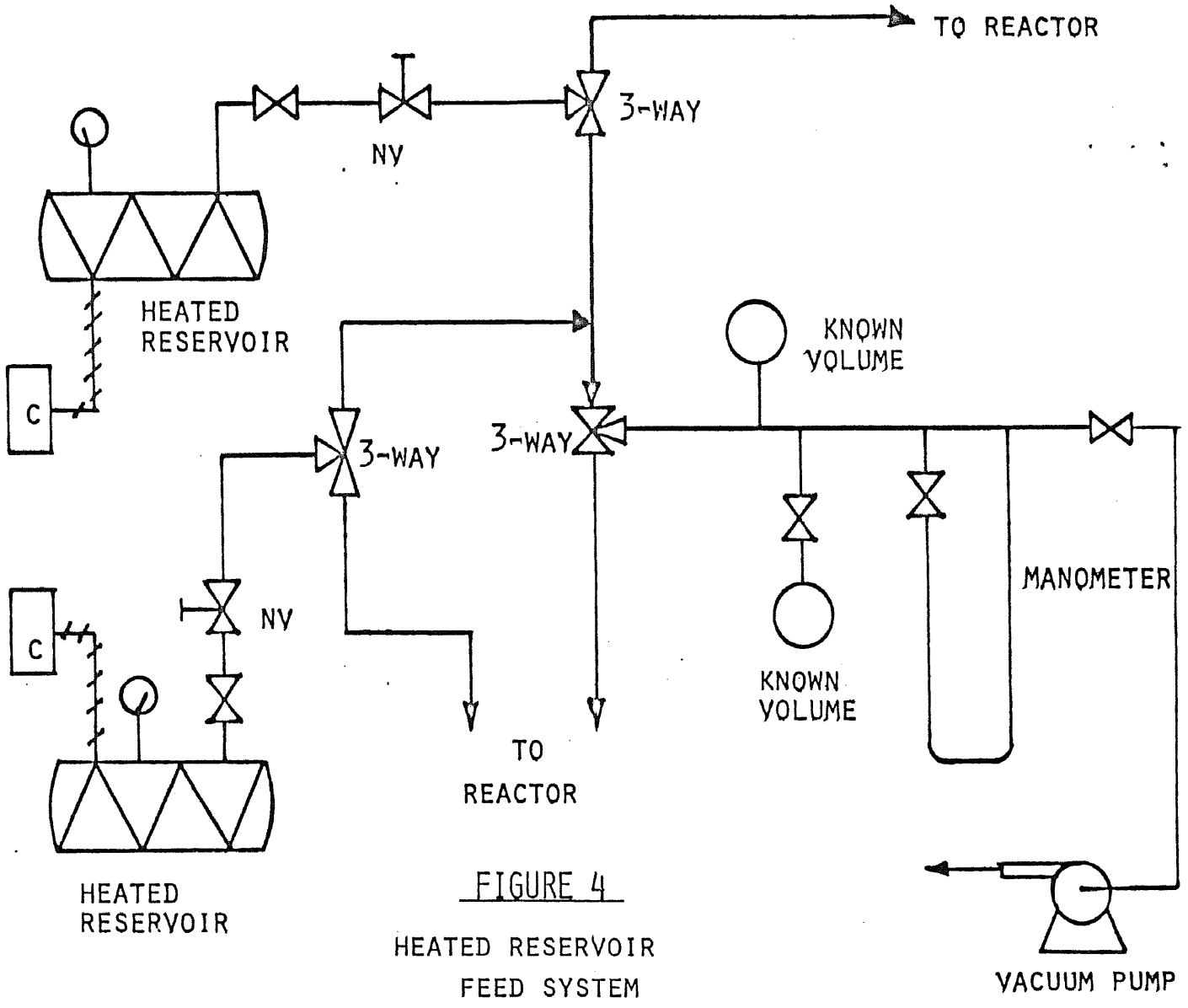

FIGURE 4

HEATED RESERVOIR
FEED SYSTEM

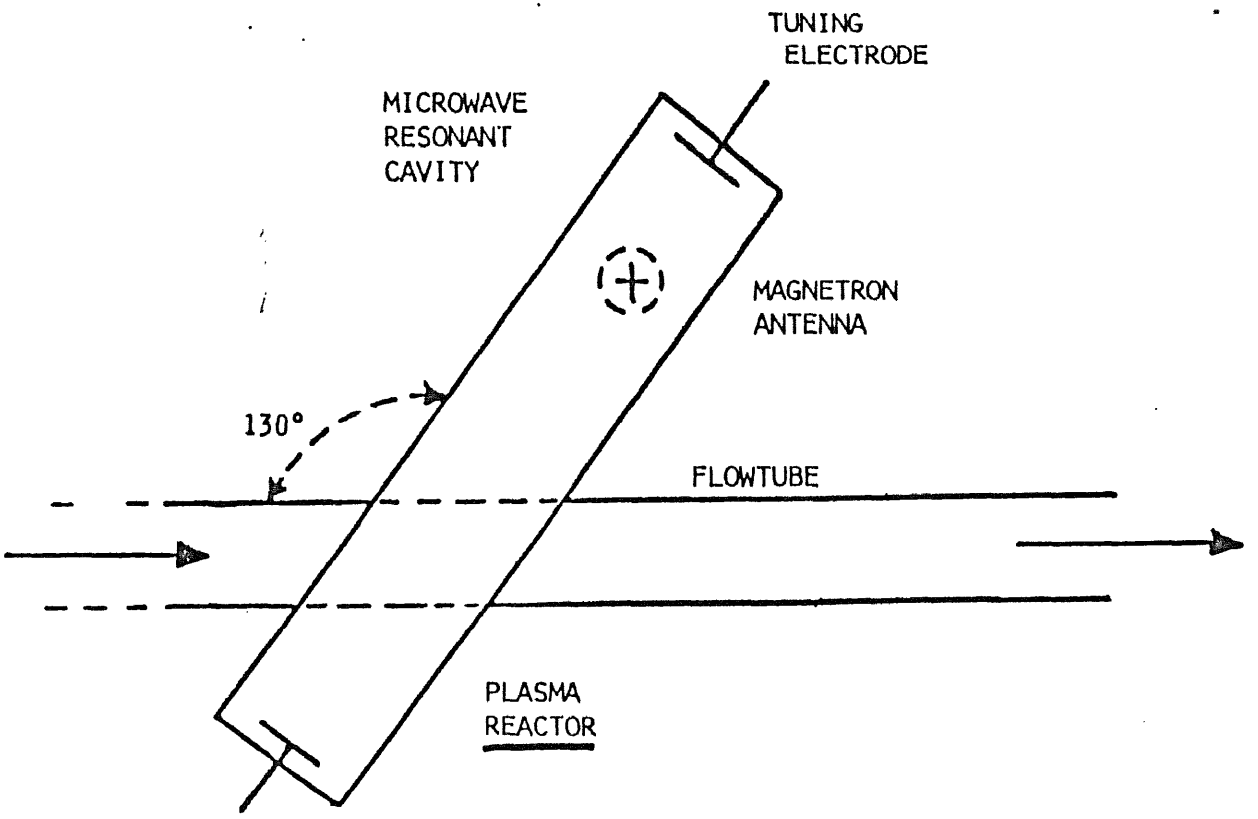

FIGURE 5

PLASMA REACTOR AND WAVEGUIDE

and power generation are described thoroughly in reference (29).

The microwave power to the plasma is controlled and varied by adjusting the input voltage to the transformer supplying the magnetron using a 0-120 volt Variac. An ammeter was placed in-line with the primary transformer and power was calculated from the known voltage and current. It is estimated that approximately 50 per cent of the input power is converted to energy in the plasma (30). The magnetron was operated in both half-wave and full-wave rectification modes. There was no observed significant difference in conversion or product distributions between the full and half-wave rectification modes for comparable input powers. Half-wave was then primarily used as it was optimum for maintaining the discharge at higher pressures due to the higher peak voltage. The full-wave mode was found to be limited to a relatively narrow pressure range (0.5 to 1.5 mm Hg) in this experimental setup.

The reactor effluent is analyzed with an on-line flame ionization detector (FID) gas chromatograph for quantitative determination of the reactant halocarbon and product halocarbon and hydrocarbon vapors. The sample is collected for this analysis by drawing reactor effluent through a 1/16 inch ID stainless steel loop which is cooled to liquid nitrogen temperature (-196°C). A schematic showing operation of this sample collection system is shown in Figure 6. The liquid nitrogen trap is sufficient to quantitatively collect the effluent material with the exception of H_2, CO, and CH_4,

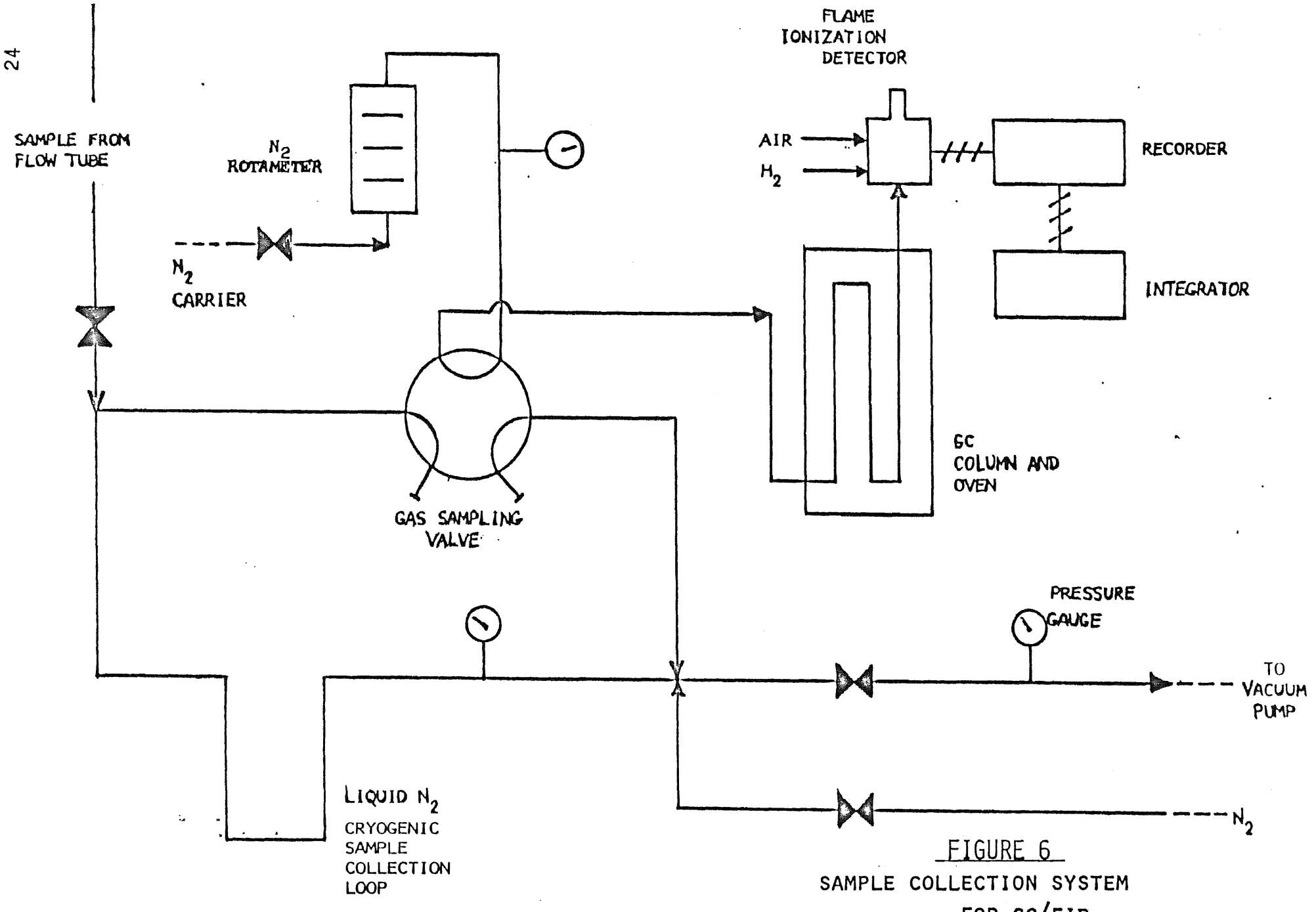

FIGURE 6

SAMPLE COLLECTION SYSTEM
FOR GC/FID

* IN SAMPLE COLLECTION MODE: TURN CLOCKWISE FOR INJECTION MODE

which have significant vapor pressures at this temperature. Sample collection (freeze trapping) is performed for a constant known fixed time, usually 40 seconds. The sample collection loop is then isolated and pressurized up from vacuum with N_2 to 5 psia. The liquid nitrogen bath is then replaced with a boiling water bath to vaporize the collected sample. The loop is further pressurized with N_2 to the operating pressure of the GC column. The sample is then injected into the GC using a heated six port gas sampling valve (Carle model Mk.11). The analytical GC column, a (1.83m X 3.18 mm) 10 per cent SP 2100 on Chromasorb W or DC 200 on Gaschrome P, is normally operated isothermally at 55°C or greater in a Carle 9500 gas chromatograph. A Hewlett-Packard 3390A integrator and a Beckman 1005 recorder are used to quantify and record the output signal respectively.

The reactor effluent is analyzed with an on-line thermal conductivity detector (TCD) gas chromatograph for quantitative determination of product carbon oxides (CO and CO_2). An evacuated volume (250 ml) on a sidearm of the main flow tube is filled with effluent to reactor pressure. It is then pressurized to 2 atmospheres with helium. A syringe sample is drawn off and injected into the analytical GC column, (1.83mm X 3.18m) with Carbosieve B or S packing. The column is operated isothermally at 80°C in a Carle 8700 gas chromatograph. A Hewlett-Packard 3390A integrator and Heath 205 recorder are used in conjunction with this GC.

Measurement of HCl is performed using either pH or specific ion electrode analysis. As with the CO_x analysis, a

known volume is filled with reactor effluent and then pressurized with helium. The mixture is then bubbled through a basic solution. The measured change in pH or chloride ion concentration in this aqueous solution permits calculation of the HCl concentration in the reactor effluent gas.

Separate reactor effluent samples are collected in a 250 ml evacuated grab sample bulb for analysis by gas chromatography/mass spectrometry (GC/MS). After filling at reactor pressure, the bulb is pressurized with helium to 2 atmospheres (200 kPa) and run on a Varian Mat 44 capillary column GC/MS for qualitative analysis of all species in the reactor product stream.

III. RESULTS AND DISCUSSION

1. Reactor Analysis

Kinetic analysis of the plasma reactor data in this study applied the ideal plug flow reactor design equation in an attempt to determine a kinetic rate expression. The preferred preliminary rate equation was that which best correlated the experimental data. This analysis provided various kinetic parameters such as reaction orders and overall rate constants.

The design equation for an ideal plug flow reactor is given by

$$V / F_{Ao} = \int_{0}^{X_{Af}} (dX_A / -r_A) \qquad (1)$$

where V = reactor volume (liter), F_{Ao} = molar feed rate of reactant A (moles/sec), X_A = conversion of A, and r_A = time rate of loss of A (mole/lit-sec). At the low pressures in the tubular fast flow reactor in this study (< 20 mm Hg), diffusion of reacting components in the radial direction is fast enough to provide a flat concentration profile across the diameter of the reactor at a given point along its length. This occurs despite the low Reynolds numbers of the total gas flow, which indicate laminar flow. A discussion of the fast flow reactor and justification for the kinetic plug flow assumption can be found in (32).

In the initial analysis efforts, the assumed rate equation has been of the form

$$-r_A = -dC_A / dt = k\, C_A^{\,a}\, C_B^{\,b} \qquad (2)$$

where k = rate constant, C_i = molar concentration of reactant i (moles/lit), and a,b are orders with respect to a given reactant. We can write

$$C_i = C_{io}\,(1-X_i) / (1+E_i\, X_i) \qquad (3)$$

where C_{io} = initial concentration of A measured at a given set of conditions, and E_i = volume expansion coefficient. Applying equation (3) for A and B to equation (2), and then susbstitution of equation (2) into equation (1) results in a system performance equation

$$(kV) \quad \frac{C_{Ao}^{\,a}\, C_{Bo}^{\,b}}{F_{Ao}} = \int_0^{X_{Af}} \frac{(1+E_A\, X_A)^{(a+b)}}{(1-X_A)^a\,(1-X_B)^b}\, dX_A \qquad (4)$$

where the volume expansion has been based on reactant A. Based on an assumed stoichiometry and initial molar feed rates, equation (4) can be reduced to a function of A only

$$\int_0^{X_{Af}} \frac{(1+E_A\ X_A)^{(a+b)}\ dX_A}{(1-X_A)^a\ (1-X_A/(PM))^b} = (kV)\ \frac{C_{Ao}^{(a+b)}\ M^b}{F_{Ao}} \qquad (5)$$

where P = the stoichiometric ratio of B to A and M = the ratio of molar feed rates of B to A. This equation takes the form of the y = mx straight line. Using experimental data on conversion X_A and initial feed rates F_{Ao} and concentration C_{Ao}, a plot of the left hand side of (5) versus $(C_{Ao}^{(a+b)}\ M^b)\ /\ F_{Ao}$ should yield a straight line of slope (kV), providing: 1) equation (2) is an accurate representation of the reaction rate, 2) orders a and b are correct, and 3) the assumed values P and E_A are correct. Taking the volume of the reactor V as the visible glow discharge region of the plasma, values of the rate constant k are determined. Due to the complexity of the integral, its evaluation was performed numerically with Simpson's Rule. Examples of the calculation of feed rates F_{Ao} and concentrations C_{Ao} from actual data are presented in Appendix 6.

2. $\underline{CHCl_3/H_2}$

The reaction of chloroform ($CHCl_3$) and hydrogen (H_2) was studied in the plasma reactor. Table 3 lists a sample product distribution of hydrocarbons and chlorocarbon species observed from the plasma reaction of $CHCl_3$ and H_2. This distribution was typical of the data observed.

Figure 7 shows the relative distribution of reactor effluent components (molar disposition of carbon in feed) as a function of $CHCl_3$ conversion. As inlet CHCl3 concentration drops, with corresponding increase in $CHCl_3$ conversion, the total hydrocarbons + graphitic carbon $C_{(s)}$ account for 90 to 95 percent of the feed carbon of the converted parent, with the remainder as byproduct chlorocarbon. Of these hydrocarbons, $C_{(s)}$ + C_1 products increase while C_2 to C_4 compounds decrease slightly with higher $CHCl_3$ conversion. The C_1 to C_2 hydrocarbons included CH_4, C_2H_2, C_2H_4, and C_2H_6. The C_6 hydrocarbon yield was small, but constant. The C_3 to C_6 species were C_3H_8, C_3H_6, C_3H_4, C_4H_6, C_4H_4, C_4H_2, and C_6H_6 with no C_5 hydrocarbons observed. The product $C_{(s)}$ is solid graphitic carbon which was found to contain less than one percent polynuclear aromatics (PNA). An accurate measurement of the amount of $C_{(s)}$ produced was not possible. Also, the high vapor pressure of CH_4 at liquid nitrogen temperature does not permit freeze trapping of all product CH_4 in the present sampling system for the FID. Therefore, both CH_4 and C(s) are determined by difference based on a carbon balance. Byproduct chlorocarbons observed included CH_3Cl, CH_2Cl_2,

TABLE 3

SAMPLE PRODUCT DISTRIBUTION

$CHCl_3 + H_2$

$CHCl_3$ Conversion = 67.6 %

$CHCl_3$ Feed Mole Percent = 3.2

PRODUCT	MOLE % OF FEED CARBON	
$C_{(s)} + CH_4$	31.8 *	
C_2H_6	1.6	
C_2H_4	1.6	
C_2H_2	5.0	
C_3H_8	1.0	C_2 to C_4
C_3H_6	1.3	Hydro-
C_3H_4	2.4	carbons
C_4H_8	0.5	= 16.0
C_4H_6	0.5	
C_4H_4	1.0	
C_4H_2	1.1	
C_6H_6	1.0	
CH_3Cl	5.5	Non-parent
C_2H_3Cl	2.9	Chloro-
C_2H_5Cl	3.3	carbons
CH_2Cl_2	6.3	= 18.0
$CHCl_3$ (unconverted)	33.2	
TOTAL	100.0	

* by difference

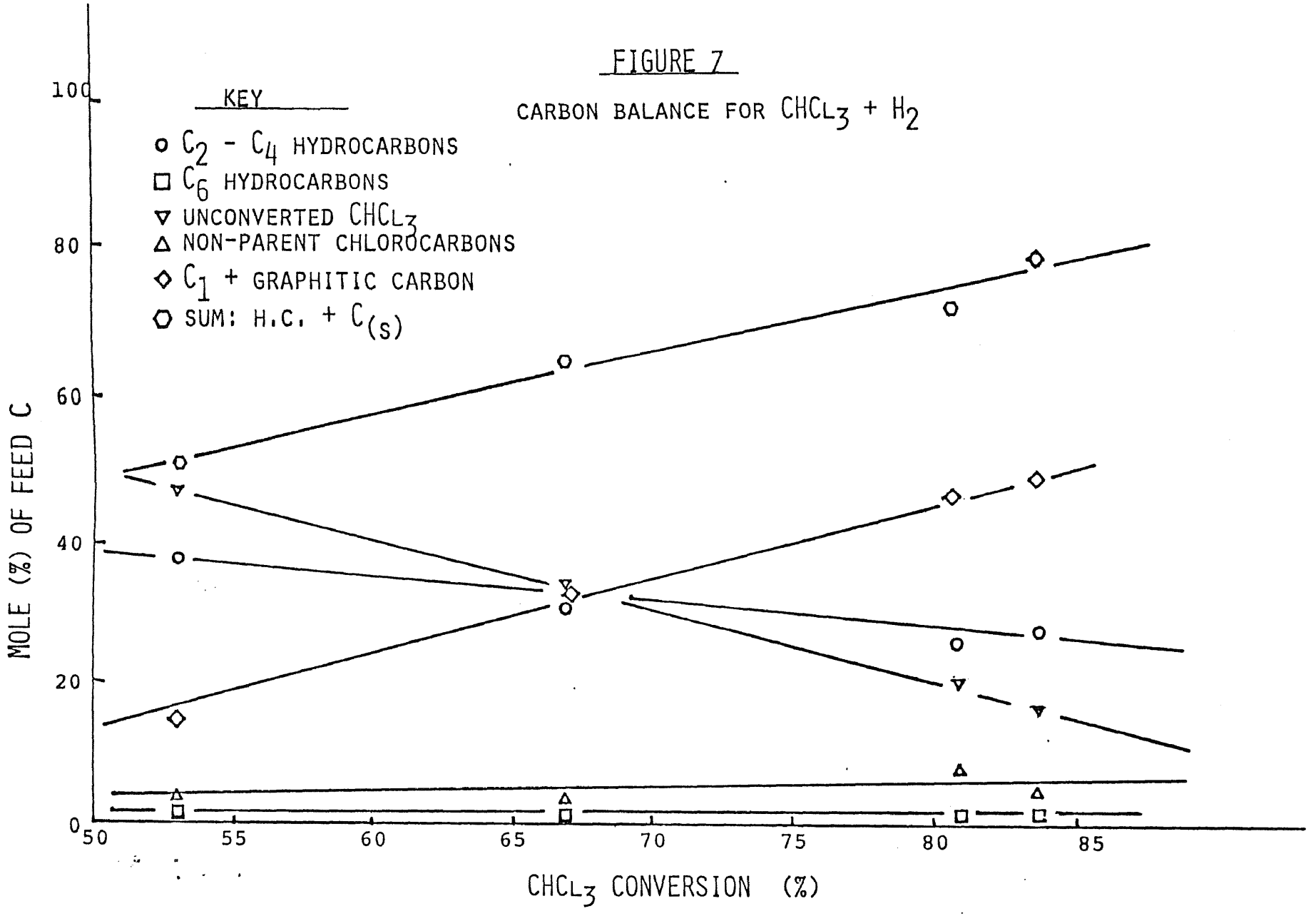
FIGURE 7
CARBON BALANCE FOR $CHCL_3 + H_2$
KEY
C_2 - C_4 HYDROCARBONS
C_6 HYDROCARBONS
UNCONVERTED $CHCL_3$
NON-PARENT CHLOROCARBONS
C_1 + GRAPHITIC CARBON
SUM: H.C. + $C_{(S)}$
MOLE (%) OF FEED C
0
20
40
60
80
100
50
55
60
65
70
75
80
85
$CHCL_3$ CONVERSION (%)

C_2H_3Cl, and C_2H_5Cl. Future efforts will better quantify CH_4 and $C_{(s)}$.

The disposition of the chlorine atoms from the feed compounds studied is of importance from the standpoint of detoxification. A relative Cl balance (molar disposition of Cl in the feed) is shown in Figure 8 for the $CHCl_3/H_2$ system. Difficulties were encountered with reproducibility in the present setup for quantitative analysis of HCl. Therefore, HCl was determined by difference with a Cl balance. However, the presence of significant quantities of HCl was confirmed qualitatively by GC/MS and the pH meter test described earlier. Chlorocarbon byproducts as well as unconverted parent were quantitatively determined by GC/FID. Independent analysis (33) for Cl in the graphitic carbon residues showed little, if any, Cl present in this byproduct. As shown in Figure (8), Cl removed as byproduct chlorocarbons accounts for 4 to 5 percent of the Cl in converted parent $CHCl_3$ over the entire conversion range obtained. Of the $CHCl_3$ converted, greater than 90 percent of the feed Cl in the converted parent is removed as HCl.

An assumed overall stoichiometry is

$$CHCl_3 + 3\ H_2 \text{ -------> } 3\ HCl + CH4 \qquad (6)$$

which has an $E_A = 0$. Numerous hydrocarbon products, as well as chlorinated species, were observed. This indicates that the stoichiometry represented by equation (6) does not precisely represent the overall reaction occuring. Other

FIGURE 8

CHLORINE BALANCE FOR $CHCL_3 + H_2$

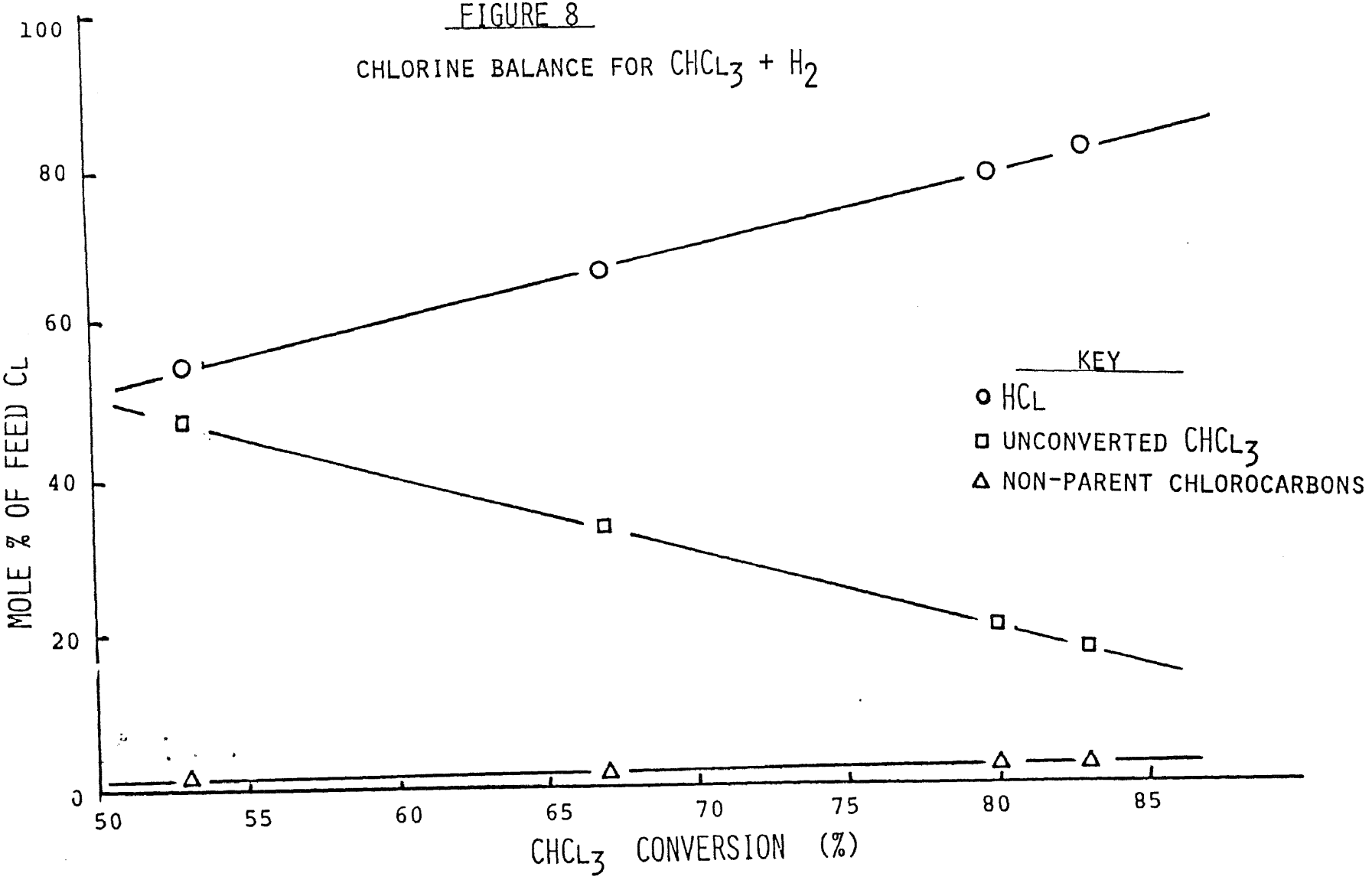

reactions can by postulated to account for each product. However, HCl and CH_4 are observed major products. Other reactions, therefore, should have a lesser impact on the kinetics. During the experiments, an increase in pressure of the reactor flow system upon initiation of the plasma was found. Since the main system vacuum pump evacuates to a given pressure for a given gas inlet rate, an increase in system pressure would indicate an increase in gas flow into the pump inlet. Therefore, an increase in pressure upon plasma initiation indicates an overall stoichiometry of more moles of product than reactant. The increase for the H_2 + $CHCl_3$ system never exceeded ten percent. A value of EA = 0.1 was therefore assumed. So equation (5) finally becomes

$$\int_0^{X_{Af}} \frac{(1+0.1X_A)^{(a+b)}\, dX_A}{(1-X_A)^a\,(1-X_A/(3M))^b} = (kV)\,\frac{C_{Ao}^{(a+b)}\, M^b}{F_{Ao}} \qquad (7)$$

Based on experimental conversion X_A and feed C_{Ao}, F_{Ao} data obtained at a constant electrical input power of 325 Watts, equation (7) yielded the best straight line fit when a = 1/2 and b = 1/2. Equation (7) then becomes

$$\int_0^{X_{Af}} \frac{(1+0.1X_A)\ dX_A}{(1-X_A)^{1/2}\ (1-X_A/(3M))^{1/2}} = (kV)\ \frac{C_{Ao}\ M^{1/2}}{F_{Ao}} \qquad (8)$$

For an estimated plasma volume V of 41.5 ml and a constant input electric power of 325 watts to the microwave power supply, the estimated empirical rate constant k is 3.2 sec^{-1}. Initial $CHCl_3$ concentrations (C_{Ao}) were calculated at the plasma reactor pressure (< 5 mm Hg) and at 25 ^{o}C. Experimental data and the regressed performance equation (8) are presented in Figure 9. Similar regression attempts for order a,b = 0,1,3/2, and 2 did not yield correlations as good as a = 1/2 and b = 1/2. Equation (8) and the straight line in Figure 9 includes the origin as a point in the regression. Ideally, equation (8) should pass through the origin. The non-zero intercept shown indicates either data scatter or that another rate expression may better represent this reaction system in the lower regions where data is not available at this time. Additional data in this regions will allow for consideration of other rate expressions. The fact that H_2 was in great excess for most data points in this system had minimal effect on the determination of 1/2 order on H_2.

A mechanism that explains the observed 1/2 order kinetic dependence on the parent $CHCl_3$ can be postulated using a series of reactions between atomic H, molecular H_2, $CHCl_3$,

FIGURE 9

KINETIC PLOT FOR $CHCl_3 + H_2$

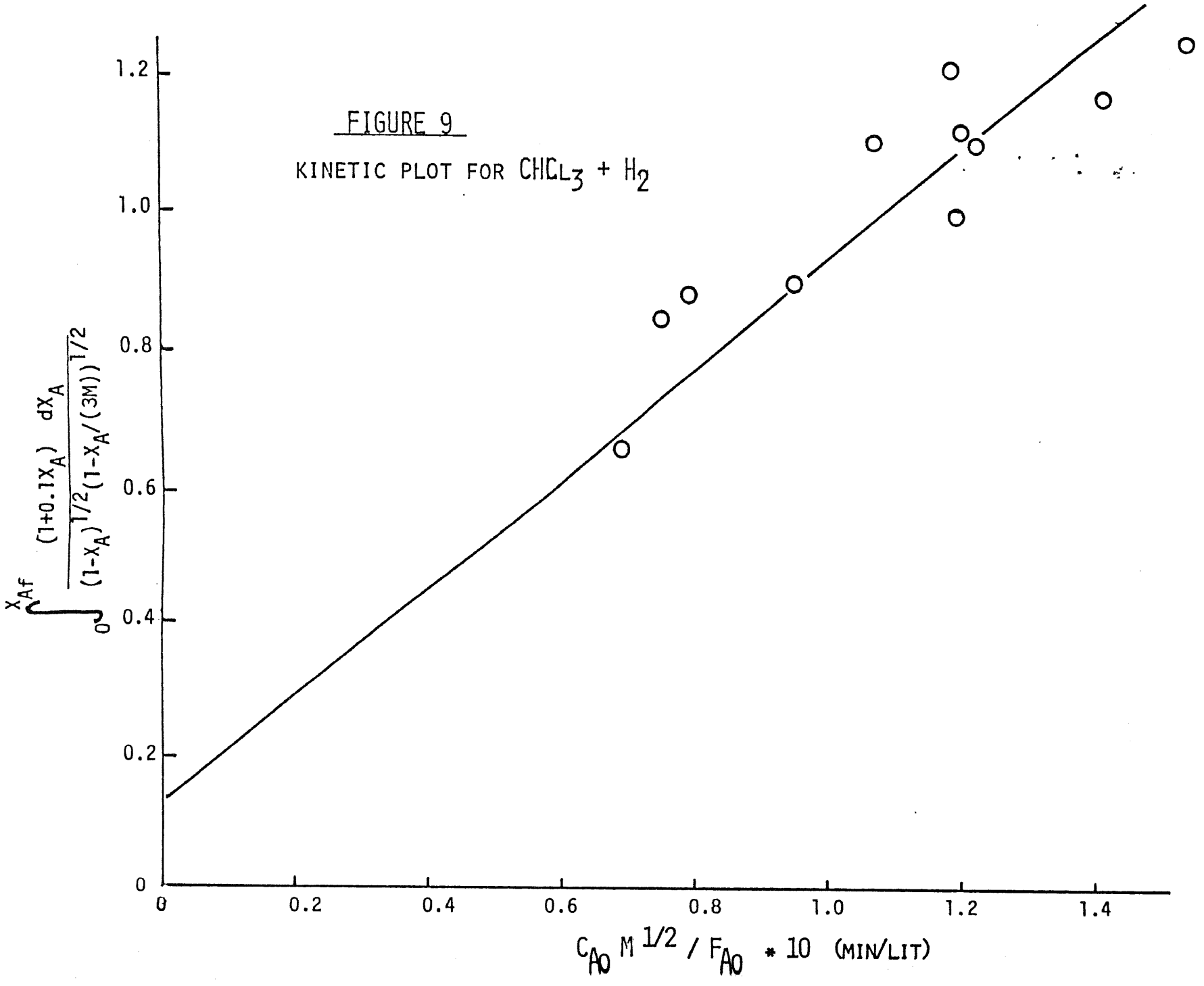

and Cl containing fragments. It emphasizes continuing abstraction and branching reactions of the chloroform fragments. One series of reactions leading to 1/2 order dependence on $CHCl_3$ is shown below:

$$e^{-*}(KE) + H_2 \xrightarrow{k_o} H\cdot + H\cdot + e^- \quad (9)$$

$$H\cdot + CHCl_3 \xrightarrow{k_1} \cdot CHCl_2 + HCl \quad (10)$$

$$H\cdot + \cdot CHCl_2 \xrightarrow{k_2} \cdot CHCl + HCl \quad (11)$$

$$H\cdot + H\cdot + M \xrightarrow{k_3} H_2 + M \quad (12)$$

$$\cdot CHCl + H \longrightarrow HCl + \cdot CH \quad (13)$$

$$\longrightarrow H_2 + \cdot CCl \quad (13a)$$

$$\cdot CCl + \cdot H \longrightarrow HCl + \cdot C \quad (14)$$

$$\cdot C + \cdot CH \longrightarrow \cdot C_2 + \cdot H \quad (15)$$

$$\cdot CCl + \cdot CCl \longrightarrow \cdot C_2Cl + \cdot Cl \quad (16)$$

$$C_2Cl + H\cdot \longrightarrow \cdot C_2 + HCl \quad (17)$$

$$\cdot CH + \cdot H + M \longrightarrow \cdot CH_2 + M \quad (18)$$

$$\cdot CH_2 + \cdot H + M \longrightarrow \cdot CH_3 + M \quad (18a)$$

$$\cdot CH_3 + \cdot H + M \longrightarrow CH_4 + M \quad (18b)$$

where species noted with a dot are free radicals and M is another molecule, such as a carrier gas molecule. Steady state approximations are made for the free radical species involved and half order dependence on $CHCl_3$ and H_2 can be

shown, based on primary reactions (9), (10), (11), and (12). Reactions (13) through (18) are subsequent reactions which probably occur and which account for some product species as well as provide the starting point for other observed products. The derivation of the half order rate law is shown in Appendix 1.

It is felt that the atomic hydrogen concentration in the plasma is controlled primarily through equilibrium reactions of the plasma with molecular hydrogen, which is in large excess, and recombination reactions of the atomic and ionic species:

$$H_2 + e^- \text{-----} > H\cdot + H\cdot + e^- \quad (19)$$

$$H_2 + e^- \text{-----} > H_2^+ + 2e^- \quad (20)$$

$$H_2 + H_2^+ \text{-----} > H_3^+ + H\cdot \quad (21)$$

$$H\cdot + H\cdot + M \text{-----} > H_2 + M \quad (22)$$

$$H_3^+ + H\cdot + e^- + W \text{-----} > 2H_2 + W \quad (23)$$

where M and W represent a third body and the wall respectively. Steady state assumptions on the H^+ ion and H free radical lead to concentrations of these substances being functions of the H_2 concentration.

Other mechanisms can be postulated to yield 1/2 order dependence on $CHCl_3$. They involve chain reactions where an active radical, generated in the plasma, reacts with the parent compound. These other mechanisms are presented in Appendix 2. One scheme has $\cdot CCl$ as the active radical in the chain propagation steps. Another uses $\cdot CCl_2$ as the propagating species. Other researchers have observed $\cdot CCl$ in

chorocarbon plasmas. Gottscho, et. al. (26) have spectroscopically observed •CCl bands, as well as Cl^+, •Cl, and Cl_2^+ in CCl_4 plasmas.

Atomic chlorine produced in this system is rapidly converted to HCl through reaction with H_2

$$\bullet Cl + H_2 \text{ <====> } HCl + \bullet H \qquad (24)$$

This is a rapid equilibrium reaction that is shifted far to the right in this system because of the high H_2 concentration. No Cl_2 byproduct was observed experimentally. The above generation of H• atoms and other reactions of H• with the parent $CHCl_3$ and its fragments are probably small perturbations on the H/H_2 equilibrium ratio established with n_2 in the discharge plasma.

Ion reactions with chloroform fragments have been omitted in the proposed mechanism above. Brown and Bell (18) indicate that ion - molecule reactions are negligable compared to free radical - molecule reactions. While ion - molecule reactions are fast (10^{-9} cm^3/sec) compared to neutral species (10^{-13} cm^3/sec), ion concentrations in the plasma are on the order of 10^{11}/ cm^3. Concentrations of free radicals are on the order of the neutral gas density (10^{17}/ cm^3) at 4 mm Hg and 300K. So rates of non - ionic reactions should be about 100 times faster than those involving ions. Hence, ion involvement was not considered in this analysis.

The observation of relatively large concentrations (several percent) of acetylene and multi-acetylenic compounds

(C_2H_2, C_3H_4, and C_4H_2) was unexpected in this hydrogen rich reaction system. These species are not unknown, however, and have been observed in fuel rich (soot producing) flames using laser induced fluorescence techniques (31). A variety of polyaromatics were also observed in such flames. The mechanisms postulated for their formation is one readily accessable in this system and probably involves the following polymerization - type reactions:

$$\cdot C_2H + \cdot H \longrightarrow C_2H_2 \qquad (25)$$

$$C_2H_2 + \cdot C_2H \longrightarrow C_4H_2 + \cdot H \qquad (26)$$

$$C_4H_2 + \cdot C_2H \longrightarrow C_6H_2 + \cdot H \qquad (27)$$

$$C_2Cl + \cdot C_2H \longrightarrow C_4H + \cdot Cl \qquad (28)$$

$$\cdot C_2H + \cdot C_2 \longrightarrow \cdot C_4 + \cdot H \qquad (29)$$

etc.

The $\cdot C_2H$, $\cdot C_2Cl$, and $\cdot C_2$ radicals are present in this system for continuation of this chain polymerization mechanism. The relatively low pressure of the reactor, 1 to 10 mm Hg, probably enhances the above chain reactions over termination or recombination reactions. Arnold, et. al. (21) observed electronically excited C_2 species from the reaction of halomethanes with atomic H. Arnold postulates that C_2^* may be formed by the reaction

$$\cdot C + \cdot CX \longrightarrow \cdot C_2^* + \cdot X \qquad (30)$$

where X = halogen or hydrogen atom and C_2^* is an electron-

ically excited C_2 species. Costes (14) observed the production of carbon atoms in a low pressure reaction of atomic H with CCl_4. Gottscho, etal (26) have observed UV emission from electronically excited C atoms in CCl_4 plasmas.

The observation of graphitic carbon in the present system, with essentially no Cl atoms found in the solid (33), makes sence in light of the large amounts of unsaturated hydrocarbons found. Clearly the C_2 species are present either as C_2, C_2H, or C_2Cl, as well as atomic carbon. We have, in essence, a situation not unlike a soot producing flame. Despite the excess of H_2 present, the greater strength of the C-C bond (140 kcal/mole for single, 170 kcal/mole for double, 230 kcal/mole for triple) over the C-H bond (80 kcal/mole) makes the production of multi-carbon compounds favorable over higher hydrocarbons once Cl is removed as H-Cl (bond strength 103 kcal/mole). (See Table 1 for bond strengths.) Since the graphitic carbon appeared as flakes on the walls of the reactor tube, it is likely that the wall acted as a site for what amounted to a "polymerization" of C or C_2 species. One of the reasons for a low pressure, low temperature microwave reactor was the hope that the graphitic carbon $C_{(s)}$ observed in the thermal reactor would be eliminated or greatly reduced. However, $C_{(s)}$ formation appears to be favorable in these systems. Further investigation of this phenomenon, with better solid yield quantification, is required.

The non-parent chorocarbon byproducts may be the result of parent molecules going through the plasma reactor with

relatively minor alterations. An example may be Cl removal on $CHCl_3$ to yield $CHCl_2$ as in reaction (10). The $CHCl_2$ radical may become stabilized by addition of H to form CH_2Cl_2 or it may continue to lose Cl atoms as shown earlier. Other chlorocarbons may be the results of radicals produced in the chain reaction mechanism which undergo stabilization. For example, C_2Cl may pick up additional H atoms to yield C_2H_3Cl. Numerous other mechanisms can be postulated. The existence of a non-chlorocarbon byproduct lends itself to the potential of product separation and recycle; or several plasma reactors in series to remove all Cl atoms as HCl.

Despite the formation of a chlorocarbon fraction (less than 10 percent of feed Cl and carbon in the converted $CHCl_3$ parent over a conversion range of 50 to 90 percent), the thermodynamically encouraging result is that at least 90 percent of the feed Cl in the converted parent converts to HCl. This was not unexpected considering the favorable H-Cl bond as discussed earlier. In a commercial scheme, the HCl can be scrubbed from the reactor effluent with a caustic solution. Removal of Cl as HCl represents a preferred route to detoxification of the parent compound.

3. C_2HCl_3/H_2

A limited set of data was taken for the plasma reaction of trichloroethylene (C_2HCl_3) and H_2. Table 4 shows the product distribution for the reaction of trichloroethylene and molecular hydrogen at a given conversion level. The products shown were typical for this reaction.

A wide range of products were observed in the effluent of the reaction $C_2HCl_3 + H_2$. Figure 10 shows the relative distribution of products, based on a molar carbon balance, as a function of C_2HCl_3 conversion. While the data is over a limited range, total hydrocarbons + $C_{(s)}$ account for about percent of the feed carbon of the parent converted, withe the remainder as byproduct chlorocarbons. There is a slight decrease of byproduct chlorocarbons with increase in parent conversion. The hydrocarbon products included C_2H_2, C_3H_8, C_3H_4, C_3H_6, C_4H_8, C_4H_2, C_4H_{10}, C_6H_6, and $C_6H_5CH_3$. No CH_4 or C_5 hydrocarbons were observed. The chlorocarbon byproducts included $CHCl_3$, C_2HCl, $C_2H_2Cl_2$, C_2Cl_4, and C_6H_5Cl. As discussed earlier, $C_{(s)}$ and HCl were obtained by difference. All other compounds in this system were quantitatively determined by GC/FID. Figure 11 presents a relative molar Cl balance. The amount of Cl as chlorocarbon byproduct remains essentially unchanged with conversion, while the yield of HCl increases. This amounts to about 90 percent of the Cl in converted parent C_2HCl_3 removed as HCl.

A potential stoichiometry is

TABLE 4

SAMPLE PRODUCT DISTRIBUTION

$C_2HCl_3 + H_2$

C_2HCl_3 Conversion = 81.2 %

C_2HCl_3 Feed Mole Percent = 3.3

PRODUCT	MOLE % OF FEED CARBON	
$C_{(s)}$	32.8 *	
C_2H_2	21.7	
C_3H_8	3.2	
C_3H_4	2.2	C_2 to C_4
C_3H_6	1.5	Hydro-
C_4H_8	1.2	carbons
C_4H_2	3.7	= 33.7
C_4H_{10}	0.2	
C_6H_6	1.2	
C_7H_8	0.2	
C_2HCl	4.1	
$C_2H_2Cl_2$	4.9	Non-parent
$CHCl_3$	3.4	Chloro-
C_2Cl_4	0.7	carbons
C_6H_5Cl	0.2	= 13.3
C_2HCl_3 (unconverted)	18.8	
TOTAL	100.0	

* by difference

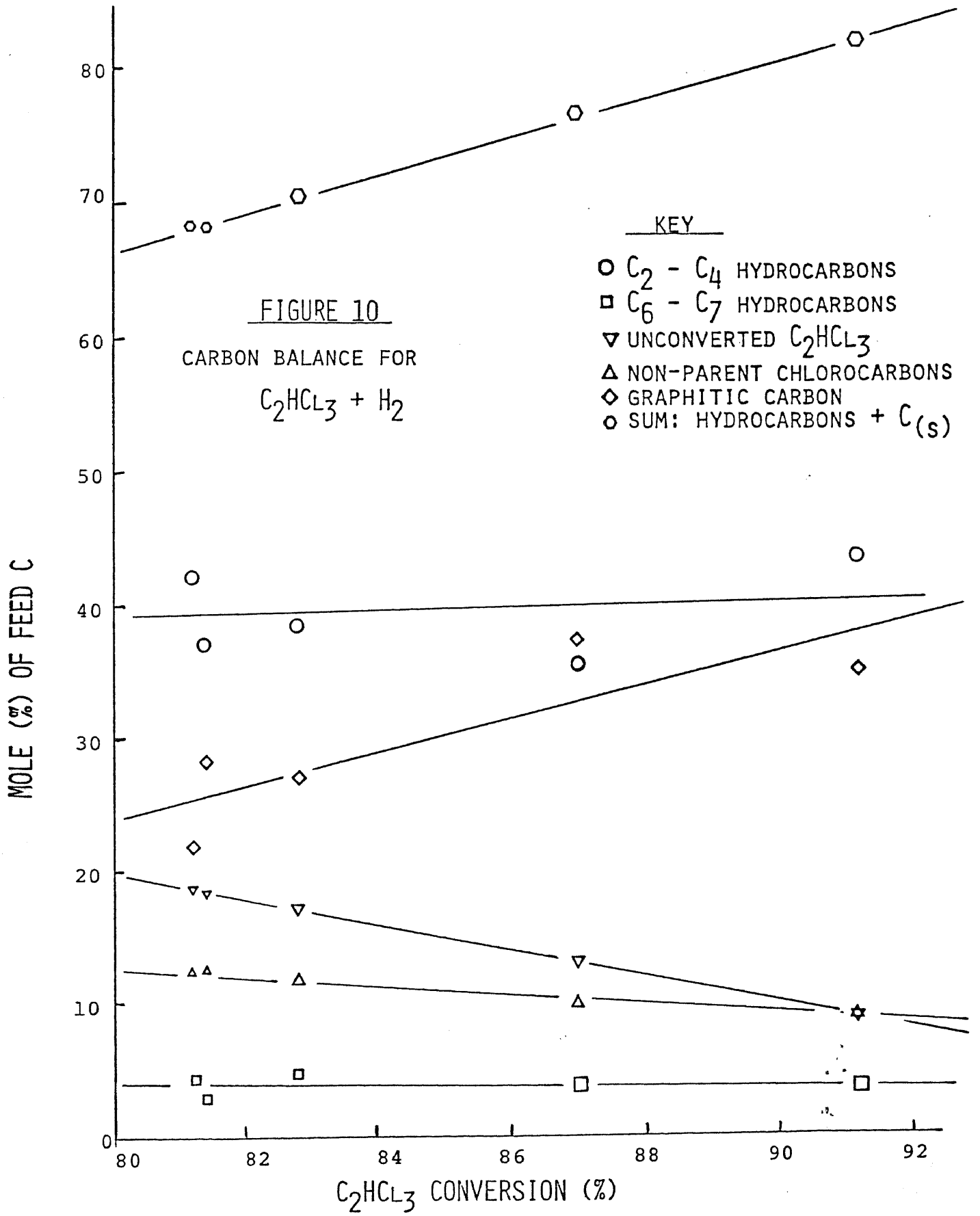

FIGURE 10

CARBON BALANCE FOR

$C_2HCL_3 + H_2$

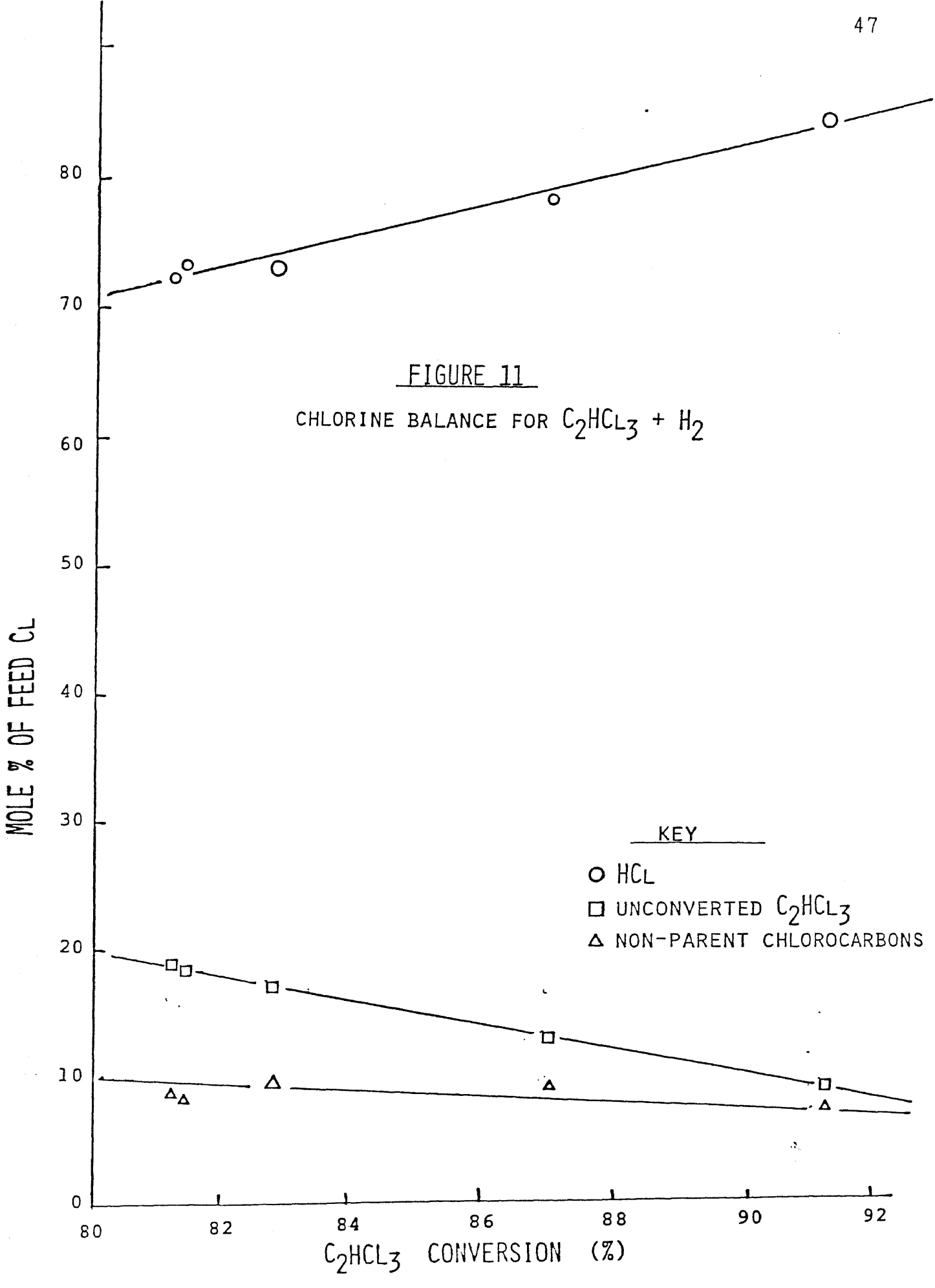

FIGURE 11

CHLORINE BALANCE FOR $C_2HCl_3 + H_2$

$$C_2HCl_3 + 2\,H_2 \text{ ------> } 3\,HCl + C_2H_2 \qquad (31)$$

with an $E_A = 0.33$. Reactor effluent analysis showed HCl and C_2H_2 among many other hydrocarbons and chlorocarbon products. Equation (31), therefore, does not adequately represent the overall reaction stoichiometry. In addition, pressure increase in the reactor upon initiation of the plasma never exceeded 5 percent. Therefore, an E_A value of 0.05 was chosen. Data regression attempts using equation (5) yielded the best correlation with a = 1/2 and b = 1/2. A plot of the regressed performance equation

$$\int_0^{X_{Af}} \frac{(1+0.05X_A)\ dX_A}{(1-X_A)^{1/2}\ (1-X_A/(2M))^{1/2}} = (kV)\ \frac{C_{Ao}\ M^{1/2}}{F_{Ao}} \qquad (32)$$

and the data are shown in Figure 12. For a plasma reaction volume of 41.5 ml and constant input electrical power to the magnetron of 325 Watts, an empirical rate constant k is found from the regression to be 5.5 sec^{-1}. Regressions with other values of a and b yielded less satisfactory correlations. As with the $CHCl_3/H_2$ system, the H_2 was often in great excess. This had a minimal effect on the determination of 1/2 order on H_2.

A mechanism to explain one-half order kinetic dependence on parent C_2HCl_3 for the reaction with H_2, which is very

FIGURE 12

KINETIC PLOT FOR $C_2HCL_3 + H_2$

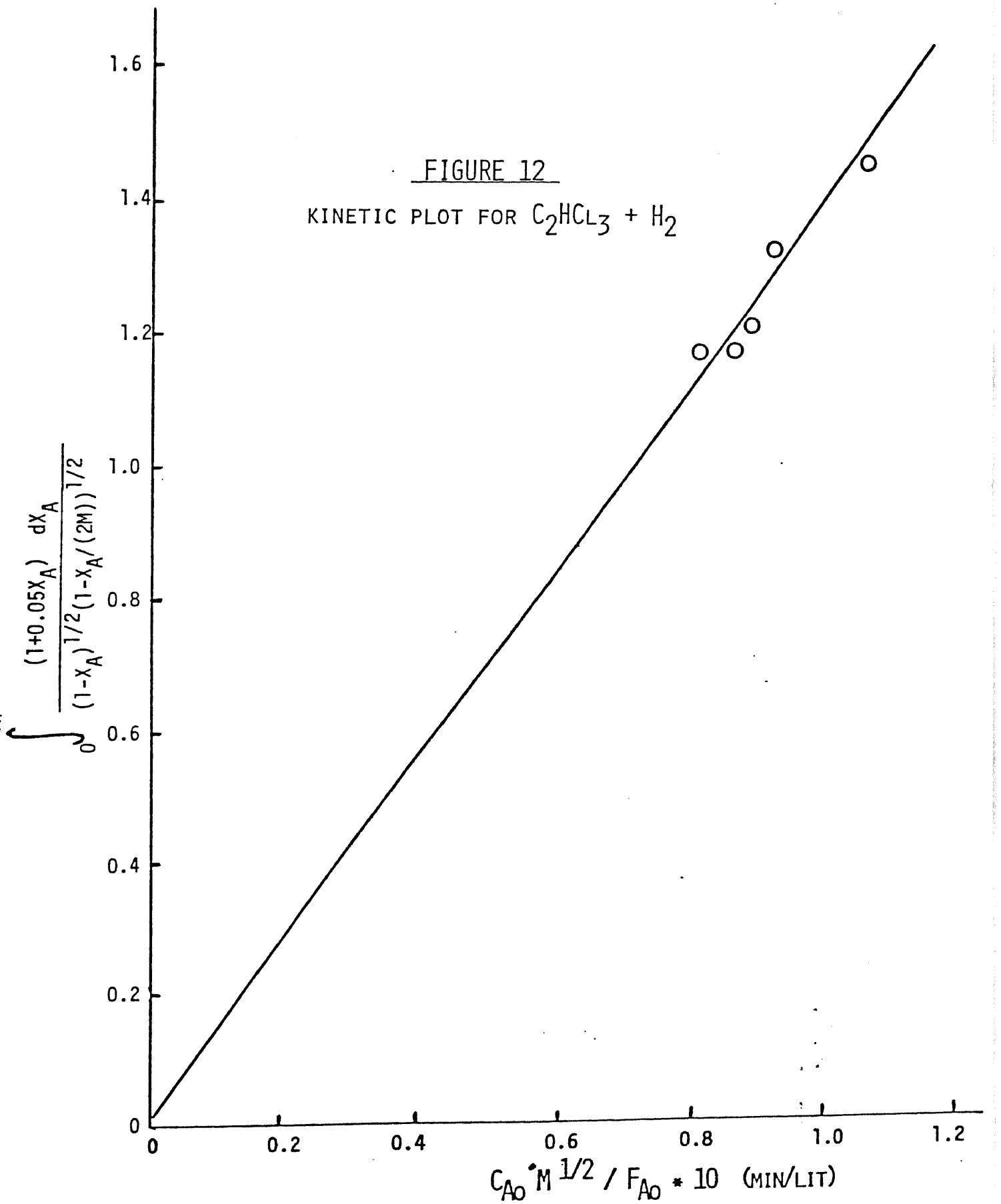

similar to that proposed for the $CHCl_3/H_2$ system, can be postulated. The parent C_2HCl_3 molecule undergoes attack by H atoms abstacting Cl to form HCl, as shown below:

$$e^- (KE) + H_2 \xrightarrow{k_o} \cdot H + H\cdot + e^- \quad (33)$$

$$H\cdot + C_2HCl_3 \xrightarrow{k_1} \cdot C_2HCl_2 + HCl \quad (34)$$

$$H\cdot + \cdot C_2HCl_2 \xrightarrow{k_2} \cdot C_2HCl + HCl \quad (35)$$

$$H\cdot + H\cdot + M \xrightarrow{k_3} H_2 + M \quad (36)$$

$$\cdot C_2HCl^* \longrightarrow \cdot Cl + \cdot C_2H \quad (37)$$

etc.

where C_2HCl^* is excited due to collision with a free electron e^- (KE) or another excited species. With the formation of various C_2 radicals, subsequent reactions involving these species to form hydrocarbon and graphitic carbon can occur, as discussed earlier with the $CHCl_3/H_2$ system. The derivation leading to 1/2 order dependence on C_2HCl_3 and H_2 is shown in Appendix 3. Appendix 4 contains an alternate mechanism which employs an active C_2Cl species as the propagating agent in a chain reaction initiated by unimolecular decomposition of an excited C_2HCl_3 molecule.

The C_2HCl_3 molecule introduces the potential added reactivity of a double bond. In addition to abstraction, an

H atom can attack the double bond in an addition reaction. Subsequent abstractions to remove Cl and additions by H may contribute to the variety of products observed. The strengths of the C-C double bond relative to the strength of the C-H bond make subsequent abstractions more likely than C-C bond fissure. Moreover, breaking the C-Cl bond (81 kcal/mole) and forming the H-Cl bond (103 kcal/mole) make abstraction of Cl by H more favorable because both H_2 and HCl are similar in bond energies. Experimental data confirmed the integrity of the C_2HCl_3 double bond in the H_2 system. Little, if any, CH_4 was observed and only small amounts of C_1 chlorocarbons were produced. By far, the dominant hydrocarbon and byproduct chlorocarbon byproducts were C_2 (or greater) unsaturated species.

A parallel mechanism leading to the observed kinetic orders for the reaction of $C_2HCl_3 + H_2$ is postulated. It emphasizes addition by H across the double bond of C_2HCl_3, but does not cause fissure of the C-C bond.

$$e^- (KE) + H_2 \xrightarrow{k_o} H\cdot + H\cdot + e^- \qquad (38)$$

$$H\cdot + C_2HCl_3 \xrightarrow{k_1} C_2H_2Cl_3 \qquad (39)$$

$$H\cdot + C_2H_2Cl_3 \xrightarrow{k_2} \cdot C_2H_2Cl_2 + HCl \qquad (40)$$

$$H + H + M \xrightarrow{k_3} H_2 + M \qquad (41)$$

$$C_2H_2Cl_2 + H \text{ -----> other reactions} \qquad (42)$$

The derivation of the observed kinetic orders, based on this mechanism, is shown in Appendix 3A. The molecule $C_2H_2Cl_2$ is dichloroethylene. In the highly reactive plasma reactor, this species can undergo subsequent abstraction reactions or addition reactions. This can also conveniently explain the observation of such byproducts as $C_2H_2Cl_2$. It is likely that this parallel mechanism contributes significantly to the conversion of C_2HCl_3.

As with the $CHCl_3/H_2$ system, the reaction of C_2HCl_3/H_2 yielded significant quantities of unsaturated compounds, especially acetylenic and multi-acetylenic compounds. A comparison of Tables 3 and 4 show that both reacting systems produce a range of C_2, C_3, and C_4 saturated and unsaturated hydrocarbons. Both yield a small benzene product and assorted non-parent chlorocarbons, but no C_5 species. The $CHCl_3/H_2$ system has a significant CH_4 yield, which was not observed in the C_2HCl_3/H_2 reaction. Conversely, the later system produced small amounts of toluene, unseen in the $CHCl_3/H_2$ system.

A comparison of Figures 7 and 10 show product trends as functions of parent conversion. Both systems yielded a small C_6 - C_7 aromatic product. Each shows a non-parent chlorocarbon byproduct yield. Over a comparable conversion range (80 to 90 percent), these chlorocarbons account for about 15 percent of the feed carbon in the converted parent in the C_2HCl_3/H_2 system and about 5 to 10 percent in the $CHCl_3/H_2$

system. Over the same conversion range, the $CHCl_3/H_2$ system shows a C_2 - C_4 hydrocarbon yield accounting for about 35 percent of the feed carbon in the converted parent. The C_2HCl_3/H_2 system produced about 45 percent. Total hydrocarbon + $C_{(s)}$ accounts for about 85 percent of the feed carbon in the converted parent for the C_2HCl_3/H_2 system, and about 90 to 95 percent for the $CHCl_3/H_2$ system, over a comparable conversion range. This is due to the slightly higher byproduct chlorocarbon yield in the C_2HCl_3/H_2 reaction.

The comparison of hydrocarbons product yields between the $CHCl_3/H_2$ and C_2HCl_3/H_2 systems reflects the relative strength of the C-C multiple bond. As discussed earlier, the presence of C_2H, C_2Cl, and C_2 radicals accounts for the high degree of unsaturated products. The strength of this bond (170 kcal/mole for double, 230 kcal/mole for triple) compared to the C-H bond (81 kcal/mole) also accounts for such production even in the presence of excess H atoms. The C_2 radicals link together in polymerization-type reactions to yield even C_6H_6, a small fraction of PNA's and graphitic carbon $C_{(s)}$. In the $CHCl_3/H_2$ system, the radical CCl, produced by successive abstraction reactions, can react with another CCl to form C_2Cl. Successive addition (recombination) of H to CCl can also explain the large yield of CH_4. In the C_2HCl_3/H_2 system, Cl abstraction by H atoms lead to C_2ClH, already unsaturated from the parent C_2HCl_3. Subsequent reactions of C_2ClH can easily lead to C_2H, C_2Cl, and C_2, thus producing the building blocks for the same type of

chain building as seen with $CHCl_3/H_2$. However, the inherent strength of the C-C multiple bond in C_2Cl makes less likely the formation of CH_4 in excess H, as evidenced by a lack of CH_4. This is also evident in the relatively lower yield of C_2 - C_4 hydrocarbons for the $CHCl_3/H_2$ system as compared to C_2HCl_3/H_2. The prevalence of the C_2Cl and C_2H radical in the later system contributes to higher yields of the acetylenic and multi-acetylenic compounds. In both systems, the strength of C-C bonds can explain the presence of graphitic carbon $C_{(s)}$. The lack of any C_5 products might be explained by the relative stability of a ring structure. As the C_2 species come together, the transition from a C_4 unsaturated linear chain to a C_6 aromatic ring is favored over the elimination a CH species to yield an ungainly and unsaturated C_5 linear molecule.

4. $\underline{C_2HCl_3/H_2O}$

Table 5 shows the product distribution for the reaction between trichloroethylene and water vapor at a given conversion level. This distribution was typical for other experimentally obtained conversion levels for this system.

The use of water vapor (H_2O) in place of H_2 represents a less expensive hydrogen source. In addition, the presence of oxygen atoms in the system introduces the prospect of product carbon oxides (CO_x). Consider the reaction of C_2HCl_3 with H_2O in the plasma reactor. (Since each species is a liquid at ambient conditions, two separate heated feed reservoirs were employed as vapor sources, as described in the Experimental Apparatus section). It was observed that a range of conversions of C_2HCl_3 sufficiently large for kinetic analysis was achieved without H_2O in significant excess over C_2HCl_3.

As in the earlier reacting system, plasma reactor products and byproducts were determined and quantified for the reaction system of C_2HCl_3 and H_2O. Figure 13 shows the relative distribution of reactor effluent components (based on molar disposition of carbon in the feed) as a function of C_2HCl_3 conversion. Total hydrocarbons + CO + $C_{(s)}$ account for 50 to 90 percent of the feed carbon of the converted parent over the conversion range studied. The remaining 50 to 10 percent was byproduct chlorocarbons. Interestingly, the C_2 to C_3 hydrocarbon yield accounts for only 20 to 10 percent of feed carbon of the converted parent over the experimental conversion range. The yield of CO + $C_{(s)}$

TABLE 5

SAMPLE PRODUCT DISTRIBUTION

$C_2HCl_3 + H_2O$

C_2HCl_3 Conversion = 97.0 %

C_2HCl_3 Feed Mole Percent = 39.2

PRODUCTS	MOLE % OF FEED CARBON	
$CO + C_{(s)}$	84.1 *	
C_2H_2	5.5	
C_2H_4	0.9	C_2 to C_3
C_2H_6	0.3	Hydro-
C_3H_4	0.5	carbons
C_3H_6	0.1	= 7.3
CH_3Cl	1.4	
CH_2Cl_2	0.8	
C_2HCl	0.7	Non-parent
C_2H_3Cl	1.1	chloro-
$C_2H_2Cl_2$	0.1	carbons
C_2Cl_4	1.4	= 5.5
C_2HCl_3 (unconverted)	3.1	
TOTAL	100.0	

* by difference

FIGURE 13

CARBON BALANCE FOR $C_2HCl_3 + H_2O$

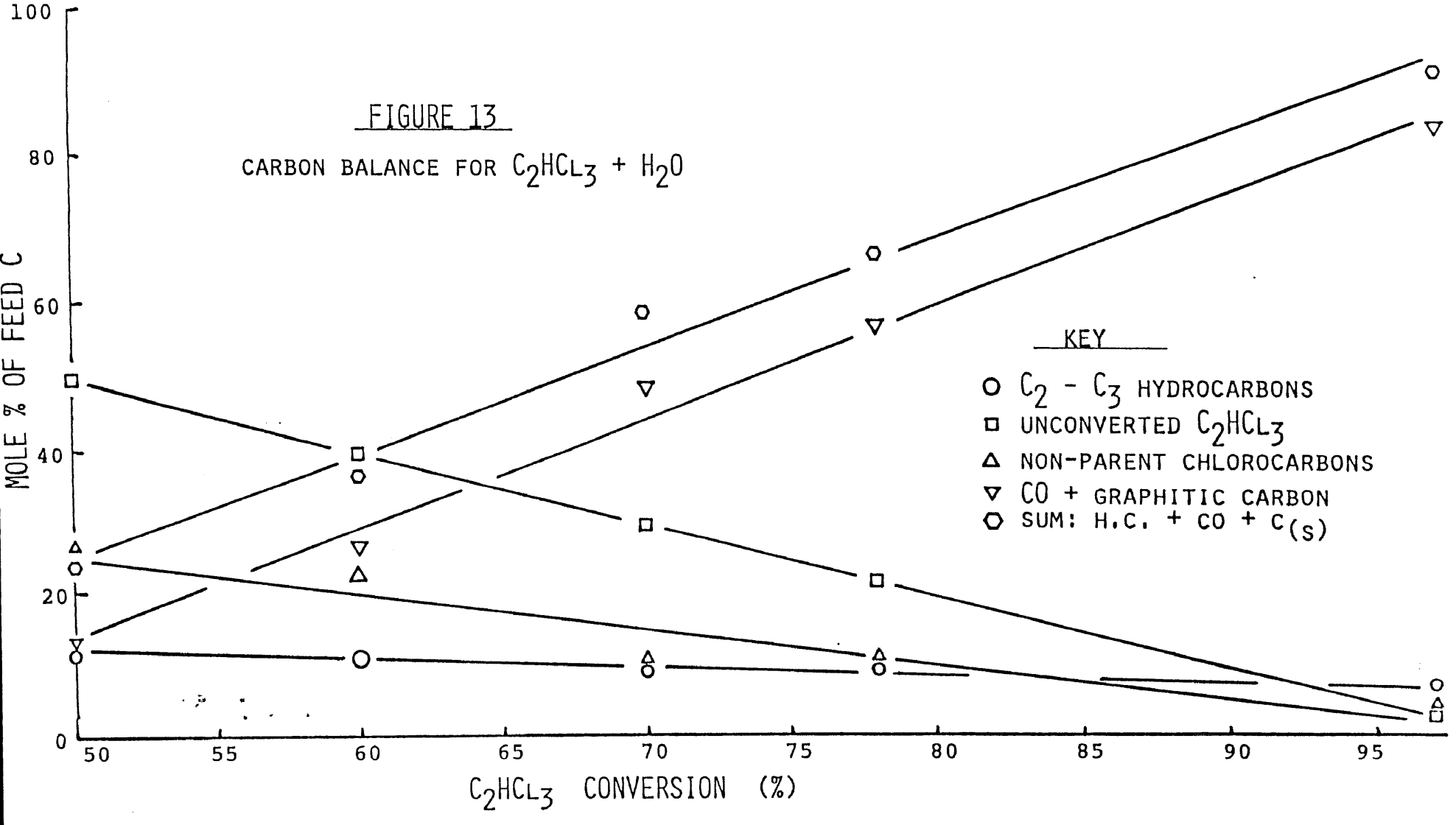

accounts for feed carbon of the converted parent with the level rising from 20 to 80 percent over the conversion range. Due to difficulties in reproducibility encountered in the present setup for quantitative CO_x analysis, the yields of $CO_x + C_{(s)}$ were found by difference based on a C balance. However, analysis by GC/TCD qualitatively showed significant CO yield, but no CO_2. The hydrocarbon and chlorocarbon yields were quantitatively determined by GC/FID. Both GC/MS and GC/TCD showed trace, if any, amounts of CH_4 yield. The C_2 to C_3 hydrocarbons included C_2H_2, C_2H_4, and C_2H_6. There were no other higher hydrocarbons in noticeable amounts. Some GC/MS runs, however, did show traces of C_6H_6. The chlorocarbon byproducts included CH_3Cl, C_2HCl, C_2H_5Cl, C_2H_3Cl, CH_2Cl_2, $C_2H_2Cl_2$, C_2HCl_3, and C_2Cl_4. Some high boiling multi-chlorinated C_5 and C_6 hydrocarbons were observed in trace amounts on some GC/MS runs. Table 5 lists the product distribution of hydrocarbon and chlorocarbon species observed at a given C_2HCl_3 conversion. This distribution of specific compounds is typical of the data observed.

Disposition of Cl in the $C_2HCl_3 + H_2O$ system followed trends similar to those found in the $CHCl_3 + H_2$ system. As shown in Figure 14, the percentage of feed Cl removed as HCl increases with C_2HCl_3 conversion. For conversion levels of approximately 65 percent or greater, HCl accounts for about 90 percent or more of the feed Cl in the converted parent. However, for conversions below 65 percent, data indicates significant feed Cl removal (of the converted parent) as

FIGURE 14

CHLORINE BALANCE FOR $C_2HCl_3 + H_2O$

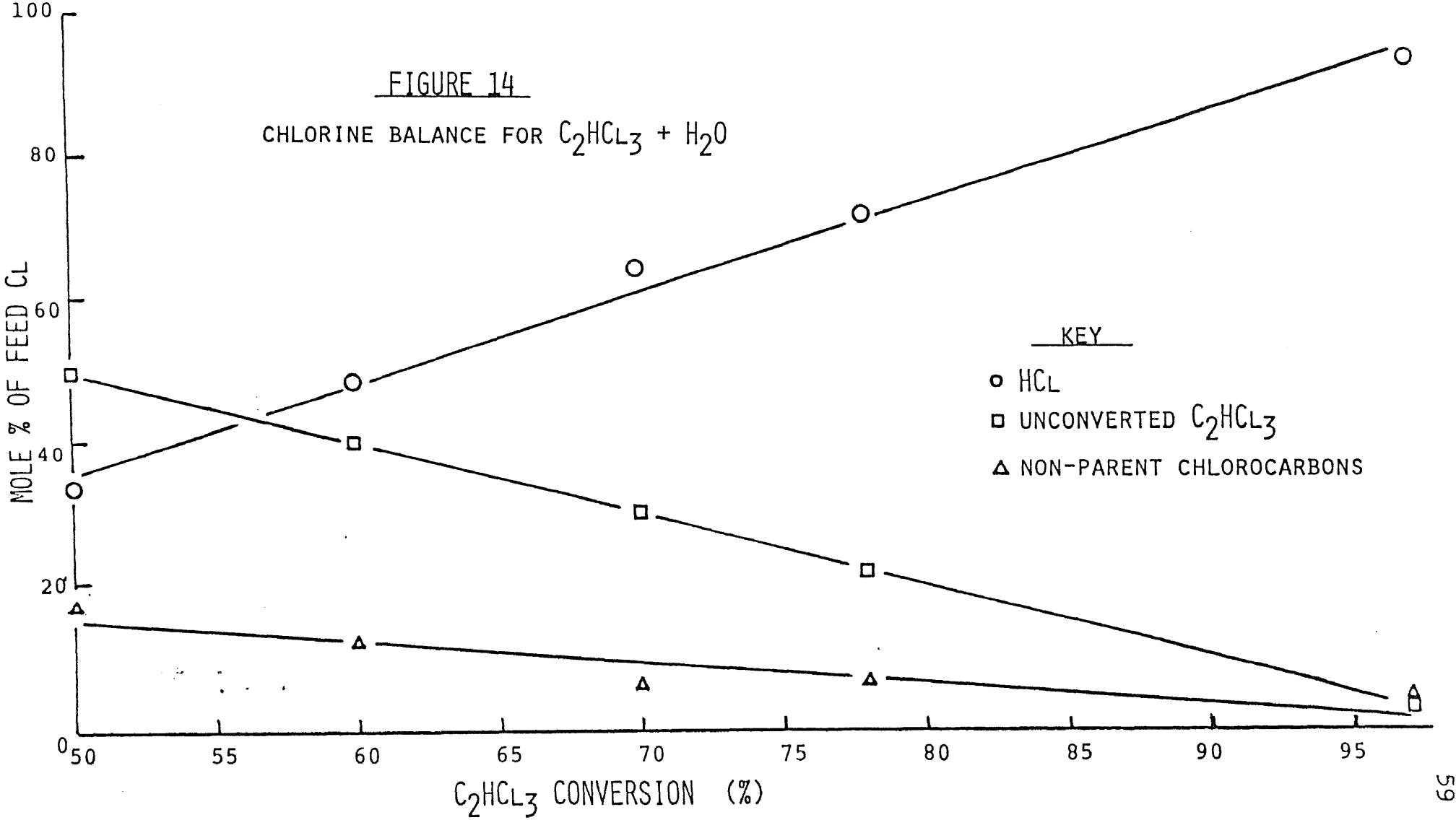

non-parent chlorocarbons. For example, at the 50 percent conversion level, about 30 percent of the feed Cl in the converted parent is removed in byproduct chlorocarbons.

A potential stoichiometry, based on observed major products, is

$$C_2HCl_3 + 3/2\ H_2O \text{ ----> } 3\ HCl + CO + 1/4\ O_2 + 1/2\ C_2H_2 \quad (43)$$

with an $E_A = 0.9$ and $P = 3/2$. It was also observed that system pressure would increase by approximately 50 percent with initiation of the plasma. This indicated a stoichiometry with significantly more moles of products than reactants. With an $E_A = 0.9$ and $P = 3/2$, the performance equation (5) becomes:

$$\int_0^{X_{Af}} \frac{(1+0.9X_A)^{(a+b)}\, dX_A}{(1-X_A)^a\,(1-X_A/(1.5M))^b} = (kV)\frac{C_{Ao}^{(a+b)}\, M^b}{F_{Ao}} \quad (44)$$

The regression which best fitted a straight line resulted from a=1/2, b=1/2. Values of 0,1,3/2,2, etc. for either a or b were less satisfactory. A plot of the regressed performance equation for a=1/2, b=1/2

$$\int_0^{X_{Af}} \frac{(1+0.9X_A)\ dX_A}{(1-X_A)^{1/2}\ (1-X_A/(1.5M))^{1/2}} = (kV)\ \frac{C_{Ao}\ M^{1/2}}{F_{Ao}} \qquad (45)$$

with experimental data points is presented in Figure 15. With a plasma volume taken to be 41.5 ml, an empirical rate constant $k = 17.\text{sec}^{-1}$ for an constant input electric power of 500 Watts to the microwave power supply. The origin was included in the regression. The small non-zero intercept can be attributed to data scatter. Initial concentrations were calculated at 25°C and the pressure of the plasma reactor. Appendix 6 describes the procedure used to calculate inlet concentrations.

The introduction of H_2O into the plasma system as a hydrogen source complicates the reaction mechanism but simplifies the product slate. In addition to H atoms, use of H_2O adds OH and O radicals to the plasma reaction. At a maximum, there are two available H atoms for every O atom. A check of bond strengths (Table 1) shows the C-C triple bond (230 kcal/mole) to be nearly as strong as the C-O bond (260 kcal/mole). The HO-H bond (119 kcal/mole) is somewhat stronger than the H-H bond (104 kcal/mole). It is postulated that the observed 1/2 order kinetic dependence on C_2HCl_3 in the C_2HCl_3/H_2O system can be explained by an addition mechanism. Radical OH attacks the double bond of C_2HCl_3 and forms what may be an epoxide intermediate. Rapid attack on

FIGURE 15

KINETIC PLOT FOR $C_2HCl_3 + H_2O$

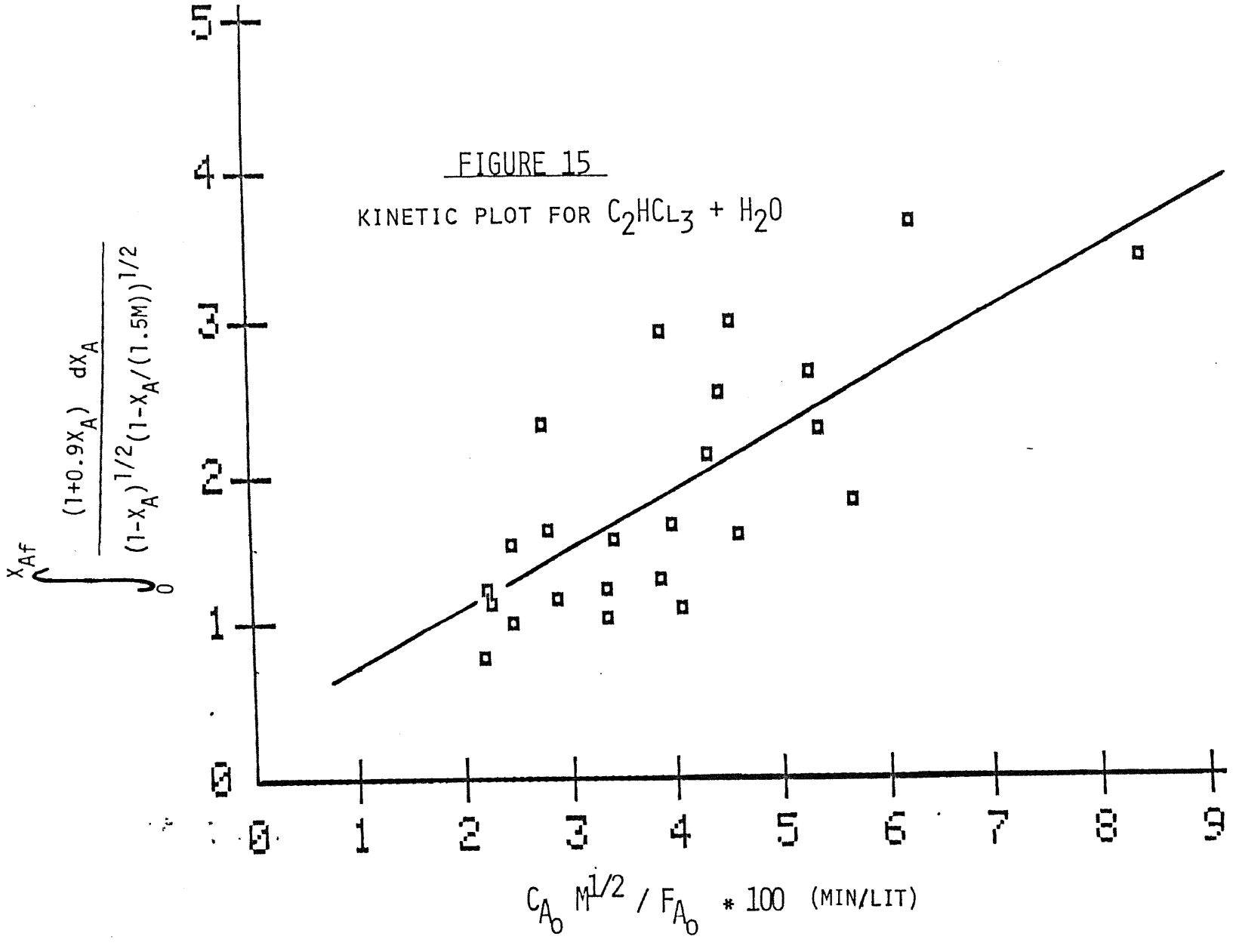

this species by a second OH removes either H or Cl to form H_2O or HOCl respectively, with the epoxide structure left intact, but probably vibrationally excited as a result of collision by a free electron or other excited species in the plasma. This epoxide then decomposes to form species which can further react with H and/or OH to form CO and HCl. The postulated mechanism is presented below:

$$e^- (KE) + H_2O \xrightarrow{k_o} \cdot OH + \cdot H + e^- \quad (46)$$

$$\cdot OH + C_2HCl_3 \xrightarrow{k_1} C_2(OH)HCl_3^{\ddagger} \quad (47)$$

$$\cdot OH + C_2(OH)HCl_3^{\ddagger} \xrightarrow{k_2} HOCl + C_2(OH)HCl_2^{\ddagger} \quad (48)$$

$$\cdot OH + C_2(OH)HCl_3^{\ddagger} \longrightarrow H_2O + C_2(OH)Cl_3^{\ddagger} \quad (48a)$$

$$C_2(OH)Cl_3^{\ddagger} \longrightarrow C(OH)Cl + \cdot CCl_2 \quad (49)$$

$$C_2(OH)HCl_2^{\ddagger} \longrightarrow C(OH)HCl + \cdot CCl \quad (49a)$$

$$\cdot OH + \cdot OH \xrightarrow{k_3} HO_2 + \cdot H \quad (50)$$

$$\cdot OH + \cdot OH \longrightarrow H_2O + \cdot O \quad (50a)$$

$$HOCl + \cdot H \longrightarrow HCl + HO\cdot \quad (51)$$

$$C(OH)Cl + H\cdot \longrightarrow HCl + \cdot OCH \quad (52)$$

$$\cdot OCH + \cdot OH \longrightarrow CO + H_2O \quad (52a)$$

$$\cdot OCH + H\cdot \longrightarrow CO + H_2 \quad (52b)$$

$$C(OH)HCl + \cdot OH \longrightarrow H_2O + C(OH)Cl \quad (53)$$

etc.

The second OH radical could also act to abstract the H atom from the first OH, after it has added across the C-C double bond in the initial attack to form the epoxide. In this case, the excited epoxide decomposes to form reactive species similar to those above. The CCl_2 radical can undergo further reactions to form CO or C_2 species to contribute to unsaturated hydrocarbons and $C_{(s)}$ formation. This will become more apparent with better quantification of CO and $C_{(s)}$ yields. The attacks by OH are rapid and efficient due to large thermodynamic favorability of the C-O bond. It should be mentioned that attack by O atoms can occur in addition to OH attack. Concentrations of O atoms can be significant due to the relative speed of the OH + OH bimolecular reaction (equation 50 and 50a). The derivation leading to 1/2 order kinetic dependence on C_2HCl_3 is presented in Appendix 5.

As mentioned, formation of OH from H_2O also gives H atoms. These H atoms can abstract Cl from a variety of species in the plasma. They may also react with parent C_2HCl_3 molecules in the Cl abstraction mechanism described in Appendices 3 and 3a. While the end products are not as thermodynamically favored as those from OH attack on C_2HCl_3 (i.e. HCl bond strength 103 kcal/mole versus CO bond strength of 260), the H mechanism for C_2HCl_3 conversion can be used to account for the small amounts of C_2 - C_3 unsaturated hydrocarbons and C_2 - C_3 chlorocarbons. This mechanism would also contribute C_2H, C_2Cl, and C_2 species for polymerization to $C_{(s)}$.

An interesting observation made in comparing the use of H_2O instead of H_2 lies in what appears to be the relative efficiency of H_2O in converting C_2HCl_3. For example, one point in the C_2HCl_3/H_2 data shows 83 percent conversion of C_2HCl_3 for an initial molar ratio of H_2 to C_2HCl_3 of 36 to 1. An 83 percent C_2HCl_3 conversion level was achieved in the H_2O system with an initial molar ratio of H_2O to C_2HCl_3 of 2 to 1. In general, for similar conversions of C_2HCl_3, the initial molar ratios in the H_2O data were under 3 to 1; whereas, the H_2 system operated at far greater ratios (about 30 to 1 or more). This suggest that H_2O is a much more effective agent to achieve C_2HCl_3 conversion than H_2 in this plasma system.

Reflection on bond strengths show that the efficiency of H_2O in converting C_2HCl_3 comes from the favorability of the C-O bond. The initial attack by OH on the C-C double bond in C_2HCl_3 to form stable C-O bonds is much more effective, due to the strength of this bond, than the initial abstraction of Cl by H to form HCl. Since the relative rates of the initial reaction is lower for the H system, higher H concentrations are needed to affect the same C_2HCl_3 conversion as with lower concentrations of OH relative to C_2HCl_3. This explains why the required molar ratios of H_2 to C_2HCl_3 were so much higher than the ratios in the H_2O runs to observe similar kinetic conversions.

While C_2HCl_3 introduces potential reactivity of the double bond, the higher activity of a H_2O + C_2HCl_3 reaction is not adequately accounted for by this. Similar conversion

levels in both the $CHCl_3/H_2$ and C_2HCl_3/H_2 systems required molar feed H_2-to-parent ratios of at least one order of magnitude greater than the ratio of H_2O to C_2HCl_3. This indicates that it was the H_2O plasma reactivity, not the double bond, that lead to faster conversions. Data for a reaction such as $CHCl_3/H_2O$ would yield added information to gauge the relative reactivity of a double bond in the parent compound in the plasma reactor. It clearly appears, at this point, that the activity of H_2O is driven by the thermodynamic favorability of CO production. The faster rates of reaction in the H_2O system, and the consequent lower initial H_2O to parent feed ratio, are evident in the experimentally determined rate constants. At similar input electric power levels (325 Watts), overall rate constants k for the $CHCl_3/H_2$ and C_2HCl_3/H_2 systems were about 3 sec^{-1} and 5 sec^{-1} respectively; whereas, the k for the C_2HCl_3/H_2O system is estimated to be about 13 sec^{-1}.

The use of H_2O as a hydrogen source simplifies the plasma reactor effluent. Comparison of Tables 4 and 5 shows that use of H_2O instead of H_2 generally reduces hydrocarbon yields in favor of CO_x. The C_2HCl_3/H_2O system yields a C_2 - C_3 hydrocarbon product, with no hydrocarbonds greater than C_3. As in the C_2HCl_3/H_2 system, the H_2O reaction showed no CH_4 product. Various C_1 and C_2 chlorocarbons were observed as a byproduct in each system.

A comparison of Figures 10 and 13 compares trends in molar carbon disposition for the C_2HCl_3/H_2 and C_2HCl_3/H_2O reactions. Over a comparable range of conversion (80 to 90

percent), the C_2HCl_3/H_2O system showed a light hydrocarbon (C_2 - C3) yield which accounted for about 10 percent of the feed carbon in the converted parent. The C_2HCl_3/H_2 system produced (C_2 - C_4) at about 45 percent. Over the same conversion range, the H_2 system yields total hydrocarbon + $C_{(s)}$ which accounts for about 85 percent of the feed carbon in the converted parent. The total hydrocarbon + $C_{(s)}$ + CO yield in the H_2O system accounted for about 90 percent. Clearly the lower make of hydrocarbons in the H_2O system is compensated by the introduction of significant quantities of CO. There was little, if any, CO_2 observed in the H_2O experiments. The competiton between oxygen species and C-C multiple bond formation limits polymerization reactions which form multi-carbon molecules. This explains the lack of any significant hydrocarbon concentrations greater than C_3 in the H_2O system.

A comparison of Figures 8, 11, and 14 show similar trends in the molar disposition of feed Cl. Over a comparable conversion range (about 80 to 90 percent), all systems dispose of about 90 to 95 percent of the feed Cl in the converted parent molecules as HCl and about 10 to 5 percent as byproduct chlorocarbons. (Over the same range, byproduct chlorocarbons accounted for about 10 to 15 percent of the feed carbon of the converted parent molecules.) These trends again point to the thermodynamic favorability of HCl as a sink for Cl, whether the H is supplied by H_2 or through H_2O. The persistence of the small fraction of byproduct chlorocarbons, even at high parent conversions, suggests that a

second stage plasma reactor feeding the effluent from the first stage and fresh injection of H_2 or H_2O may be necessary to completely remove all Cl as HCl. An alternative might be product separation of the reactor effluent to remove useful material such as HCl and hydrocarbons + CO from byproduct chlorocarbons. The chlorocarbons could then be recycled to supplement the fresh chlorocarbon feed to the reactor.

In a commercial operation, the $C_{(s)}$ graphitic carbon residue can be removed by intermittent shut-off of the chlorocarbon feed and plasma operation with only steam in the H_2O system or oxygen in the H_2 system. Such a procedure would effectively gasify the carbon to CO_x.

5. C_6H_5Cl/H_2

As a first step toward a potential PCB feed, the stable, halogenated aromatic mono-chlorobenzene (C_6H_5Cl) was reacted with H_2 in the plasma reactor. The C_6H_5Cl was fed using H_2 impingers. Due to the low vapor pressure of C_6H_5Cl at ambient conditions, feed concentrations were very low. This resulted in very high conversions (> 98 percent), thus precluding a kinetic analysis. However, reactor effluent analysis showed that HCl was the only Cl containing product. As shown in Figure 16, the $C_{(s)}$ + C_1 to C_2 relative product accounts for about 62 percent of the feed carbon. The C_3 to C_5 yield accounted for about 32 percent. The C_6 to C_7 products accounted for about 5 percent. The remaining 1 percent is unconverted parent, not shown in the figure. The C_1 to C_2 products included CH_4, C_2H_2, and C_2H_4. The C_3 to C_5 products were C_3H_8, C_3H_6, C_3H_4, C_4H_8, C_4H_6, C_4H_4, C_4H_2, and C_5H_8. The C_6 to C_7 compounds were benzene and toluene. Table 6 shows a typical product distribution found for the reaction of C_6H_5Cl and H_2.

At the low C_6H_5Cl feed concentrations involved, conversions exceeded 98 percent. The molar ratio of Cl to C atoms in C_6H_5Cl is low. Therefore, Cl removal as HCl was complete. The interesting result, as Figure 16 shows, lies with the destruction of the aromatic ring structure. Essentially more than 95 percent of the aromatic rings were disrupted into linear saturates and unsaturates, along with graphitic $C_{(s)}$. This demonstrates that a microwave or radio frequnecy (RF)

FIGURE 16

CARBON BALANCE FOR $C_6H_5CL + H_2$

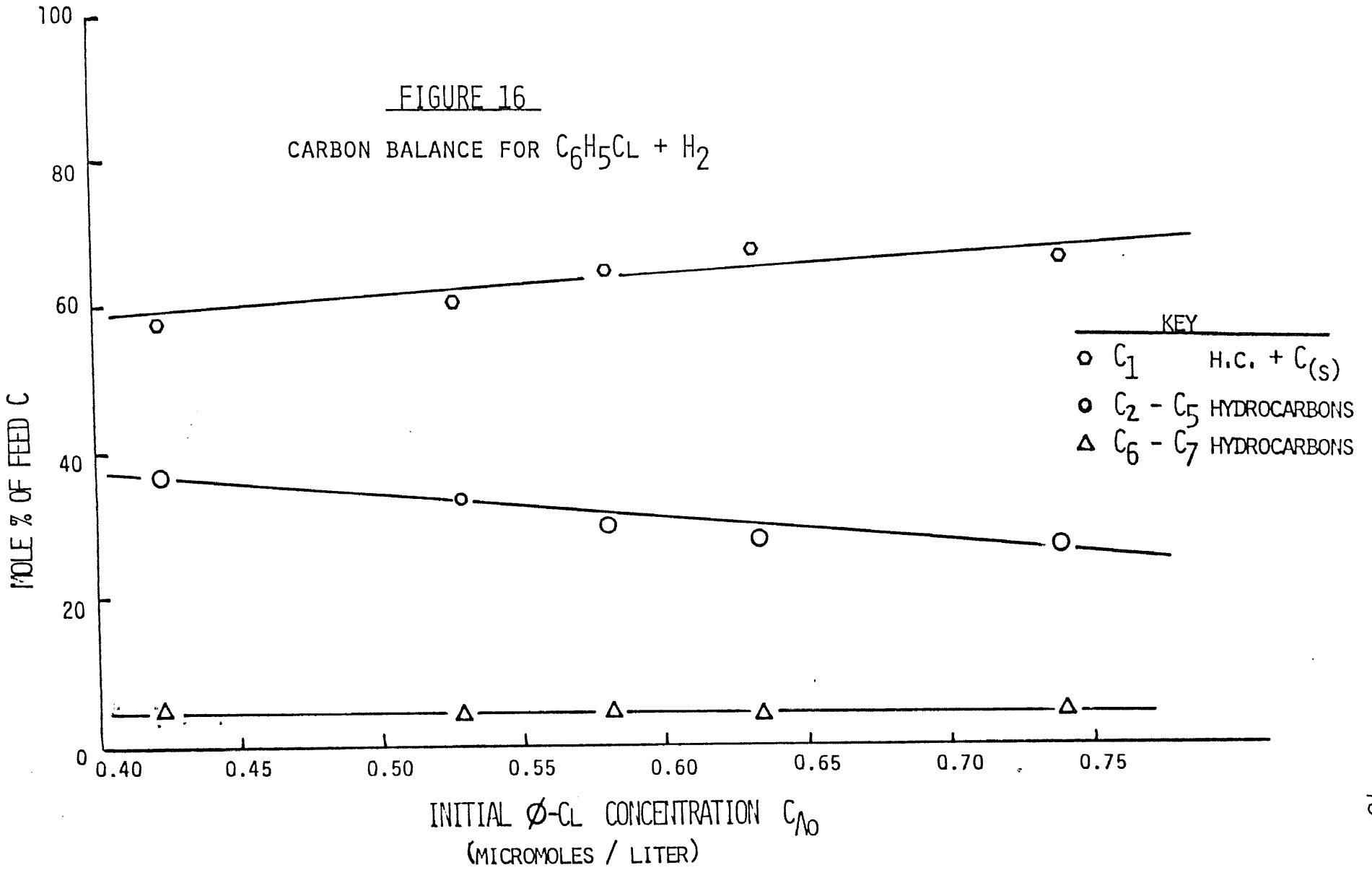

TABLE 6

SAMPLE PRODUCT DISTRIBUTION
$C_6H_5Cl + H_2$

C_6H_5Cl Conversion = 99.7 %

C_6H_5Cl Feed Mole Percent = 1.5

PRODUCT	MOLE % OF FEED CARBON	
$C_{(s)} + CH_4$	67.8 *	
C_2H_4	3.3	
C_3H_8	7.3	
C_3H_6	3.0	
C_3H_4	6.6	C_2 to C5
C_4H_8	1.6	Hydro-
C_4H_6	1.1	carbons
C_4H_4	1.1	= 27.5
C_4H_2	1.8	
C_5H_8	1.7	
C_6H_6	3.6	
C_7H_8	0.4	
C_6H_5Cl (unconverted)	0.3	
TOTAL	100.0	

* by difference

plasma reactor will efficiently serve to fragmentize and destroy aromatic ring systems. These reactors, therefore, are potentially very effective at destruction of PCB's, Dioxins, and PNA's. With Cl removal as HCl, and H or OH/O removing feed carbon atoms as hydrocarbons and/or CO, the present system offers a significant potential for conversion of toxic substances to recoverable and useful products.

F. An Arrhenius Form for the Kinetic Rate Constants

The average system energy present in the microwave plasma is a complex summation of populated levels of translational, rotational, vibrational, and electronic energies. They are unmeasureable in the classic sense, because the energies are not statistically distributed, as in a Boltzmann case. They are pumped by the interactions of atoms, free radicals, and molecules with the high kinetic energy free electrons and ions. These charged species are accelerated by the oscillating electric field of the microwaves, causing them to have high kinetic energy. A measure of temperature, as with a thermocouple, would not represent a good measure of the plasma energy. The work of Bell and Brown (18), for example, shows the energetic influence of free electrons on the chemical reactions under consideration. They observed a "kinetic steady state" for the reaction $CO + 1/2\ O_2 = CO_2$ in a radio frequency plasma flow tube reactor. Compositions corresponding to equilibrium temperatures that were higher than measured gas temperatures in the plasma were observed. This was attributed to the reactivity of high kinetic energy free electrons in the plasma.

A measureable handle on the plasma system energy is the electric energy input to the microwave generator. As discussed earlier, electric power input to the primary transformer of the magnetron was measured. This electric power input can be considered proportional to the average plasma energy through a conversion efficiency (30).

Temperature in a reacting system is traditionally related to kinetics through the Arrhenius equation

$$k = k_o * \exp(-E/RT) \quad (54)$$

This temperature is a measure of average thermal energy which can be described by a statistical distribution such as Boltzmann. For an ideal gas, the average translational kinetic energy is related to temperature by

$$0.5 * m * v^2 = (1.5 * R/N) * T \quad (55)$$

where m = mass (kg), v = average linear velocity (meter/sec), N = Avogadro's number (6.023×10^{23}/mole), and R = Gas constant (8.314 joule/mole-K). We can generalize the Arrhenius equation to allow the rate constant k to be expressed as a function of "average energy" of the plasma.

$$k = k_o * \exp(-E / \text{aver. energy}) \quad (56)$$

In the plasma system, even though the energies are non-Boltzmann, we can still approximate the Arrhenius equation by using the measured electric energy input as a handle on average energy. For the plasma reactor, we can apply a Arrhenius-type equation in the form of

$$k = k_o * \exp(-E / \text{electric power input}) \quad (57)$$

because the average energy of the plasma reaction system may be taken to be proportional to the power input through the plasma. It follows that, should equation (57) hold true, then

$$\ln k = \ln k_o - E / (\text{electric power input}) \qquad (58)$$

A plot of experimentally determined k values as a function of electric power input, related by equation (58), is shown in Figure 17. The k values were obtained from performance equation (8) using conversion data obtained as a function of input electric power for a given feed rate. The electric power input was varied and measured using the Variac and voltmeter/ammeter assembly respectively as previously described in the Experimental Apparatus section. The plot of ln k versus 1 / Watts (input) correlates very well as a straight line. A slope giving E = 174 joules/second is obtained. With the respective feed $CHCl_3$ and H_2 rates of 4.8 and 46.5 micromoles/second used, E is converted to 830 kcal/mole of feed. Now, assuming a constant efficiency, the energy of the plasma equals the product of efficiency and electrical power input. We can then rewrite equation (57) as

$$k = k_o * \exp (- E * \text{eff} / \text{P.E.})$$
$$= k_o * \exp (- E_p / \text{P.E.}) \qquad (59)$$

where P.E. is the average plasma energy and E_p can be considered an empirical activation energy for the plasma reaction with the given flows. If we assume then a 50

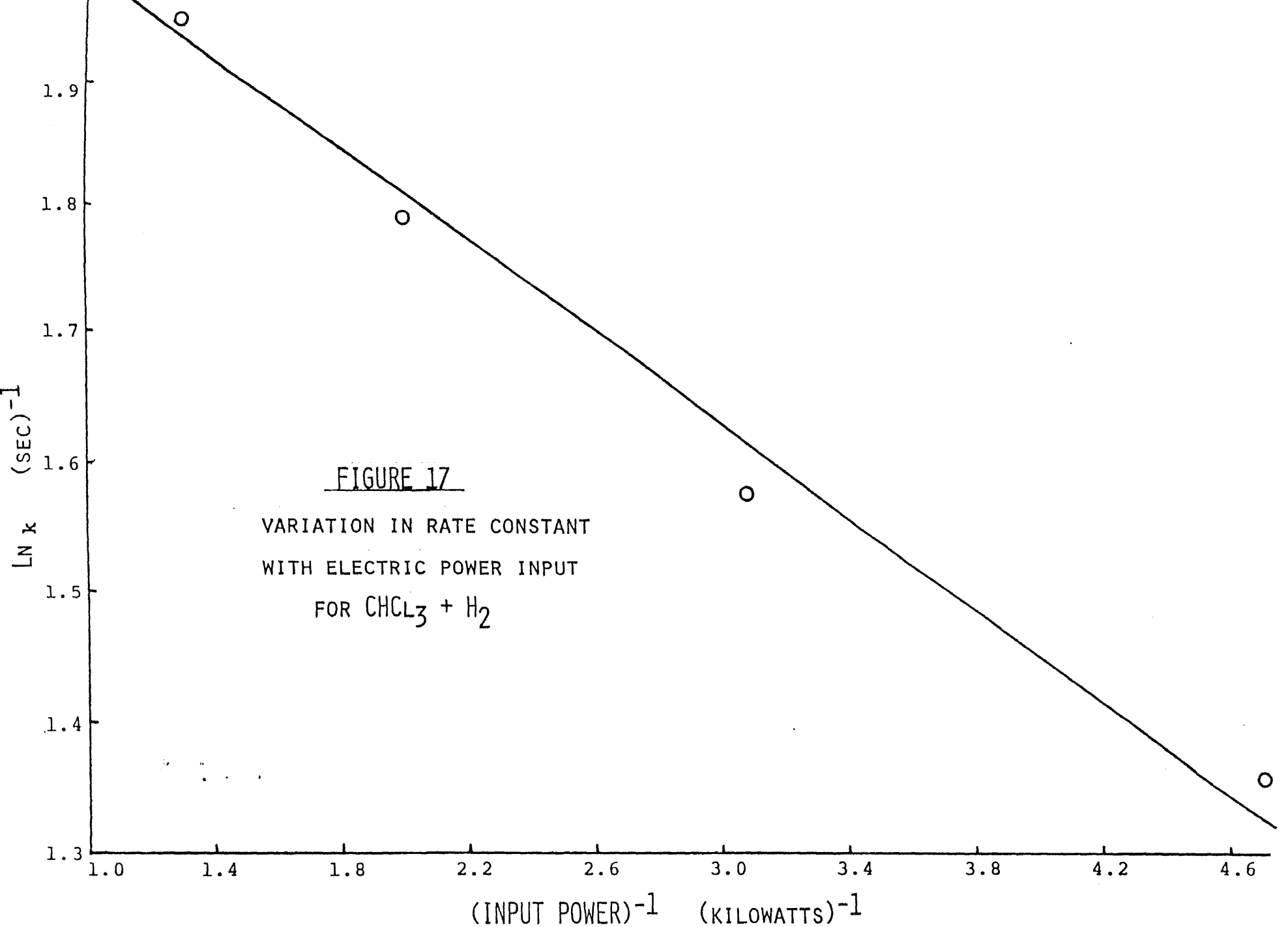

FIGURE 17

VARIATION IN RATE CONSTANT WITH ELECTRIC POWER INPUT FOR $CHCL_3 + H_2$

percent conversion efficiency of electrical power input to plasma energy (30), the E_p becomes about 410 kcal/mole of feed.

Standard activation energies for reactions may be on the order of 50 to 100 kcal/mole. The difference may represent energy going to excitation of various species in the plasma which do not contribute to reactor conversion efficiency. An example is an electronic excitation of a product molecule via a collision with a high kinetic energy electron. This molecule may then emit a visible light (i.e. glow discharge) photon which does not contribute to the conversion process.

The k values obtained using equation (8) directly, with a single data point at each power, are not as precise as obtaining k values from a number of data points obtained at each power input level. However, this is acceptable since it is the slope E of equation (58) above which is of interest. It is felt that the E as obtained here is acceptable. In addition, the favorable correlation of the data shows that an Arrhenius-type character exists for the reactions. The energy of the plasma reactor can, therefore, be controlled, with an exponential effect on reaction rate being the consequence.

IV. CONCLUSIONS

The experiments performed to date prove the applicability of reacting toxic chlorinated hydrocarbons with molecular hydrogen or water vapor in a microwave plasma discharge reactor. Through such a scheme, detoxification occurs by removal of Cl as thermodynamically favorable HCl. The reactions systems studied were $CHCl_3/H_2$, C_2HCl_3/H_2, C_2HCl_3/H_2O, and C_6H_5Cl/H_2.

The reactivity of the microwave plasma reactor was demonstrated by achieving conversions of selected parent chlorocarbons over a range from approximately 50 percent to almost 100 percent. This reactivity did not require the significant feed preheat and high temperature reactor operation required for adequate conversions in a conventional thermal reactor system. Instead, the uniqueness of the plasma reactor lies with the high density of free electrons and energetic species inherent in a plasma.

Reactions of the $CHCl_3$ and C_2HCl_3 in the presence of H_2 yielded significant quantities of HCl, a range of C_1 to C_6 light hydrocarbons, small amounts of non-parent chlorocarbons, and solid graphitic carbon. The observation of a high degree of unsaturation in the hydrocarbon products and the graphitic carbon points to the apparently high reactivity of C and C_2 radicals, which are produced in these systems, even in excesses of hydrogen. The relative strength of the carbon-carbon multiple bond is also evident in the lack of observed CH_4 in the C_2HCl_3/H_2 system. However, CH_4 was

observed in the $CHCl_3/H_2$ reaction.

Reaction of C_2HCl_3 with H_2O yielded significant quantities of HCl, only small amounts of C_2 to C_3 hydrocarbons (many unsaturated), solid graphitic carbon, and large amounts of CO. The appearance of and graphitic carbon is likely accounted for by the high reactivity of C_2 radical species on the wall of the reactor.

All reacting systems studied, with the exception of the chlorobenzene, produce non-parent chlorocarbon byproducts which generally account for about 15 mole percent or less of the of the carbon and chlorine in the converted parent for parent conversions of 80 percent or greater. Chlorocarbon byproducts account for a greater percentage of the converted parent at lower conversion levels. It is postulated that such byproducts are formed by partial alteration of the parent molecules in mechanisms parallel to the major conversion schemes. Such a byproduct suggest either a partial recycle or second stage plasma reaction in a commercial detoxification application. The amount of byproducts formed indicates that generally 85 mole percent or greater of the Cl in the converted parent forms thermodynamically favorable HCl for parent conversion levels of 80 percent or more. It is likely that the C_6H_5Cl/H_2 system did not produce any chlorocarbon byproducts because of the very low Cl/C atomic ratio in this compound relative to $CHCl_3$ or C_2HCl_3.

The microwave plasma reactor appears to be effective in disrupting aromatic ring structures. In the chlorobenzene/

H_2 effectively 95 percent of the aromatic rings were disrupted to lower linear hydrocarbon molecules. This suggests that such a plasma system may effective in the detoxification of such substances as PCB's, Dioxins, and DDT with ring disruption to simpler hydrocarbons and Cl removal as HCl.

Preliminary kinetic analysis indicate a one-half order dependence on both the parent chlorocarbon and either molecular H_2 or H_2O. Empirical rate constants, as well as the orders for these rate expressions, were determined from regression of data fitted to plug flow performance equations. For the $CHCl_3/H_2$ and C_2HCl_3/H_2 systems, the respective rate constants are 3 sec^{-1} and 5 sec^{-1} at constant input electrical power of 325 Watts. For the $CHCl_3/H_2O$ system, the rate constant is 17 sec^{-1} at a constant 500 Watts input electrical power. A kinetic rate constant for the C_6H_5Cl/H_2 system could not be obtained because data was obtained over only a very limited range of conversions.

Mechanisms describing the observed kinetic dependencies are postulated. The $CHCl_3/H_2$ and C_2HCl_3/H_2 systems employ an abstraction mechanism, wherein H atoms remove Cl atoms from the parent compound in the rate determining steps. A likely parallel mechanism for the C_2HCl_3/H_2 system considers addition a H atoms across the C-C double bond. The C_2HCl_3/H_2O system uses an addition mechanism, wherein OH or O attacks the carbon-carbon bond in the parent species. For comparable parent chlorocarbon conversion, the H_2 systems generally required an initial molar feed ratio, H_2/chloro-

carbon, about an order of magnitude greater than the H_2O /chlorocarbon ratios. This, combined with the higher rate constant for the H_2O system at comparable constant electric power input levels, point to the higher reactivity of H_2O plasma systems leading to the formation of the highly stable and energetically favorable C=O bond.

The plasma reactor was found to exhibit an Arrhenius-type rate constant, with electrical power input to the microwave generator in place of temperature. The plasma reactivity, therefore, can be varied by varying power input, which, in turn, controls the average energy of the plasma.

APPENDIX

1. $CHCl_3 + H_2$ Mechanism

One series of reactions leading to 1/2 order dependence on $CHCl_3$ is shown below:

$$e^- (KE) + H_2 \xrightarrow{k_o} \cdot H + \cdot H + e^- \quad (1)$$

$$H\cdot + CHCl_3 \xrightarrow{k_1} \cdot CHCl_2 + HCl \quad (2)$$

$$H\cdot + \cdot CHCl_2 \xrightarrow{k_2} \cdot CHCl + HCl \quad (3)$$

$$H\cdot + H\cdot + M \xrightarrow{k_3} H_2 + M \quad (4)$$

The rate of initial abstraction of Cl by H is much slower than subsequent abstractions. In fact, (2) may be aided if the parent $CHCl_3$ is excited from a collision with an energetic free electron. Since $k_1 << k_2$, eqs. (2) and (3) can be combined to form

$$2\ H\cdot + CHCl_3 \xrightarrow{k_1'} 2\ HCl + \cdot CHCl \quad (5)$$

with k_1' on the order of k_1. A steady state analysis on H results in

$$d(H)/dt = 0 = k_o(H_2) - k_1'(H)^2(CHCl_3) - k_3(H)^2 \qquad (6)$$

Since k_1 is slow, reaction (2) is rate limiting and

$$r_A = d(CHCl_3)/dt = -k_1(H)(CHCl_3) \qquad (7)$$

From eq. (6),

$$(H)^2 = \frac{k_o\,(H_2)}{k_1'\,(CHCl_3) + k_3} \qquad (8)$$

Assuming that $k_3 << k_1'(CHCl_3)$, eq. (8) reduces to

$$(H) = (k_o/k_1')^{1/2}\,(H_2)^{1/2}\,(CHCl_3)^{-1/2} \qquad (9)$$

Substitution of eq. (9) into eq. (7) results in a rate expression with the experimentally observed orders

$$r_A = d(CHCl_3)/dt = -k_1(k_o/k_1')^{1/2}\,(H_2)^{1/2}\,(CHCl_3)^{1/2} \qquad (10)$$

2. $CHCl_3 + H_2$ Alternate Mechanism

An alternative mechanism for the reaction $CHCl_3/H2$ resulting in a rate expression showing 1/2 order kinetic dependence in $CHCl_3$ is presented below. It relies on a chain reaction with an active propagating CCl radical for conversion of parent $CHCl_3$.

$$e^- (KE) + CHCl_3 \xrightarrow{k_1} HCl + CCl_2 + e^- \quad (1)$$

$$CCl_2 + H \xrightarrow{k_2} HCl + CCl \quad (2)$$

$$CCl + CHCl_3 \xrightarrow{k_3} CClH + CCl_3 \quad (3)$$

$$CClH + H \xrightarrow{k_4} H_2 + CCl \quad (4)$$

$$CClH + CClH \xrightarrow{k_5} C_2ClH_2 + Cl \quad (5)$$

$$CCl + CCl \xrightarrow{k_6} C_2Cl + Cl \quad (6)$$

Reactions (1) and (2) are chain initiation and transfer steps. Reactions (3) and (4) are chain propagation steps. Reactions (5) and (6) are chain termination steps in that carbon products formed here go on to yield stable products. The balance equation for $CHCl_3$ is

$$d(CHCl_3)/dt = -k_1(CHCl_3) - k_3(CCl)(CHCl_3) \quad (7)$$

where $k_1 = k_1'(e^-)$ and (e^-) is constant for a given power input. Steady state approximations are made for (CCl), (CCl_2), and (CClH).

$$d(CCl)/dt = 0 = k_2(CCl_2)(H) - k_3(CCl)(CHCl_3) + k_4(CClH)(H) - k_6(CCl)^2 \quad (8)$$

$$d(CCl_2)/dt = 0 = k_1(CHCl_3) - k_2(CCl_2)(H) \quad (9)$$

$$d(CClH)/dt = 0 = k_3(CCl)(CHCl_3) - k_4(CClH)(H) - k_5(CClH)^2 \quad (10)$$

Since $(CHCl_3)$ and (H) are much greater than (CCl), equation (8) reduces to

$$0 = k_2(CCl_2)(H) - k_3(CCl)(CHCl_3) + k_4(CClH)(H) \quad (11)$$

Adding eqs. (11) and (10) results in

$$0 = k_2(CCl_2)(H) - k_5(CClH)^2 \quad (12)$$

From eq. (9) we have

$$(CCl_2) = k_1(CHCl_3)/k_2(H) \quad (13)$$

Substitute eq. (13) into eq. (12) to get

$$(CClH) = (k_1(CHCl_3)/k_5)^{1/2} \quad (14)$$

Substitute eq. (13) and eq. (14) into eq. (11) to obtain

$$(CCl) = k_1/k_3 + (k_4/k_3)(H)(k_1/k_5)^{1/2}(CHCl_3)^{-1/2} \quad (15)$$

Assuming that the rate of propagation is much greater than the rate of initiation, $k_3 >> k_1$, eq. (15) reduces to

$$(CCl) = (k_4/k_3)(H)(k_1/k_5)^{1/2}(CHCl_3)^{-1/2} \quad (16)$$

Also assuming that $k_3(CCl) >> k_1$ reduces eq. (7) to

$$d(CHCl_3)/dt = -k_3(CCl)(CHCl_3) \quad (17)$$

Finally, substituting eq. (16) into eq. (17) results in

$$d(CHCl_3)/dt = -k"(H)(CHCl_3)^{1/2} \quad (18)$$

where $k" = k_4(k_1/k_5)^{1/2}$. We can include the follwing reactions involving H_2 and H

$$e^- (KE) + H_2 \xrightarrow{k_o} H + H + e^- \quad (19)$$

$$H + H + M \xrightarrow{k_7} H_2 + M \quad (20)$$

A steady state balance can now be written for (H)

$$d(H)/dt = 0 = k_o(H_2)-k_2(H)(CCl_2)-k_4(H)(CClH)-k_7(H)^2 \qquad (21)$$

If we assume that $k_7(H)^2$ and (H_2) are greater than the other terms in eq. (21) due to the excess of H_2, then eq. (21) results in

$$(H) = (k_o(H_2)/k_7)^{1/2} \qquad (22)$$

Substitution of eq. (22) into (18) finally results in a rate expression with the observed kinetic orders

$$d(CHCl_3)/dt = -k"_o\ (H_2)^{1/2}(CHCl_3)^{1/2} \qquad (23)$$

where $k"_o = k_4(k_1k_o/k_5k_7)^{1/2}$.

Another alternative mechanism is very similar to the above with the exception that this employs the CCl_2 radical as the major propagating species.

$$e^- (KE) + CHCl_3 \xrightarrow{k_1} HCl + CCl_2 + e^- \qquad (1)$$

$$CCl_2 + H \xrightarrow{k_2} HCl + CCl \qquad (2)$$

$$CCl + CHCl_3 \xrightarrow{k_3} CCl_2 + CHCl_2 \qquad (3)$$

$$CCl + CHCl_3 \xrightarrow{k_{3a}} CHCl + CCl_3 \qquad (3a)$$

$$CHCl_2 + H \xrightarrow{k_4} HCl + CHCl \qquad (4)$$

$$CCl_2 + CCl_2 \xrightarrow{k_5} C_2Cl_3 + Cl \qquad (5)$$

$$CHCl + CHCl \xrightarrow{k_{5a}} C_2H_2Cl + Cl \qquad (5a)$$

$$CCl_2 + CHCl_3 \xrightarrow{k_6} CHCl_2 + CCl_3 \qquad (6)$$

$$H + CCl_3 \xrightarrow{k_7} HCl + CCl_2 \qquad (7)$$

$$CCl + CCl \xrightarrow{k_8} C_2Cl + Cl \qquad (8)$$

The balance equation for $CHCl_3$ is

$$d(CHCl_3)/dt = -k1(CHCl_3) - k_3(CCl)(CHCl_3) - k_6(CCl_2)(CHCl_3) \qquad (9)$$

where $k_1 = k_1'(e^-)$ and (e^-) is constant for a given power input. Steady state approximations are made for (CCl), (CCl_2), and (CCl_3).

$$d(CCl)/dt = 0 = k_2(CCl_2)(H) - k_3(CCl)(CHCl_3) - k_8(CCl)^2 \qquad (10)$$

$$d(CCl_2)/dt = 0 = k_1(CHCl_3) - k_2(CCl_2)(H) + k_3(CCl)(CHCl_3) - k_5(CCl_2)^2$$

$$-k_6(CCl_2)(CHCl_3) + k_7(H)(CCl_3) \qquad (11)$$

$$d(CCl_3)/dt = 0 = k_6(CCl_2)(CHCl_3) - k_7(CCl_3)(H) \qquad (12)$$

Since $(CHCl_3)$ and (H) are much greater than (CCl), equation (10) reduces to

$$0 = k_2(CCl_2)(H) - k_3(CCl)(CHCl_3) \qquad (13)$$

From eq. (13) we get

$$(CCl) = k_2(CCl_2)(H)/k_3(CHCl_3) \qquad (14)$$

From eq. (12) we have

$$(CCl_3) = k_6(CCl_2)(CHCl_3)/(k_7(H)) \qquad (15)$$

Substituting eq. (12) and eq. (13) into eq. (9) gives

$$0 = k_1(CHCl_3) - k_5(CCl_2)^2 \qquad (16)$$

From eq. (16) we now have

$$(CCl_2) = (k_1/k_5)^{1/2}(CHCl_3)^{1/2} \qquad (17)$$

Substituting eq. (17) into eq. (14) gives

$$(CCl) = k_2(H)(k_1/k_5)^{1/2}/(k_3(CHCl_3)^{1/2}) \qquad (18)$$

Substitution of eq. (15) and eq. (16) into eq. (7) results in

$$d(CHCl_3)/dt = -k_1(CHCl_3) - k'(H)(CHCl_3)^{1/2} - k''(CHCl_3)^{1/2} \quad (19)$$

where $k' = k_3^{1/2}k_2(k_1/k_5)^{1/2}$ and $k'' = k_6(k_1/k_5)^{1/2}$.

If we assume that $k'(H) >> k''$ and k_1, then eq. (19) finally reduces to

$$d(CHCl_3)/dt = -k'(H)(CHCl_3)^{1/2} \quad (20)$$

As in the previous mechanism, development of an equation for (H) results in eq. (20) showing 1/2 order dependence on each of H_2 and $CHCl_3$.

3. $C_2HCl_3 + H_2$ Mechanism

One series of reactions leading to 1/2 order dependence on C_2HCl_3 is shown below:

$$e^- (KE) + H_2 \xrightarrow{k_o} H + H + e^- \qquad (1)$$

$$H + C_2HCl_3 \xrightarrow{k_1} C_2HCl_2 + HCl \qquad (2)$$

$$H + C_2HCl_2 \xrightarrow{k_2} C_2HCl + HCl \qquad (3)$$

$$H + H + M \xrightarrow{k_3} H_2 + M \qquad (4)$$

The rate of initial abstraction of Cl by H is much slower than subsequent abstractions. In fact, eq. (2) may be aided if the parent C_2HCl_3 is excited from a collision with an energetic free electron. Since $k_1 << k_2$, eqs. (2) and (3) can be combined to form

$$2\,H + C_2HCl_3 \xrightarrow{k_1'} 2\,HCl + C_2HCl \qquad (5)$$

with k_1' on the order of k_1. A steady state analysis on H results in

$$d(H)/dt = 0 = k_o(H_2) - k_1'(H)^2(C_2HCl_3) - k_3(H)^2 \qquad (6)$$

Since k_1 is slow, reaction (2) is rate limiting and

$$r_A = d(C_2HCl_3)/dt = -k_1(H)(C_2HCl_3) \qquad (7)$$

From eq. (6),

$$(H)^2 = \frac{k_o\,(H_2)}{k_1'\,(C_2HCl_3) + k_3} \qquad (8)$$

Assuming that $k_3 << k_1'(C_2HCl_3)$, eq. (8) reduces to

$$(H) = (k_o/k_1')^{1/2}\,(H_2)^{1/2}\,(C_2HCl_3)^{-1/2} \qquad (9)$$

Substitution of eq. (9) into eq. (7) results in a rate expression with the experimentally observed orders

$$r_A = d(C_2HCl_3)/dt = -k_1(k_o/k_1')^{1/2}\,(H_2)^{1/2}\,(C_2HCl_3)^{1/2} \qquad (10)$$

3a. $C_2HCl_3 + H_2$ Parallel Mechanism

A parallel series of reactions leading to 1/2 order dependence on C_2HCl_3 is shown below:

$$e^- (KE) + H_2 \xrightarrow{k_o} H + H + e^- \quad (1)$$

$$H + C_2HCl_3 \xrightarrow{k_1} C_2(H)HCl_3 \quad (2)$$

$$H + C_2(H)HCl_2 \xrightarrow{k_2} C_2H_2Cl_2 + HCl \quad (3)$$

$$H + H + M \xrightarrow{k_3} H_2 + M \quad (4)$$

The rate of initial addition by H to the double bond is much slower than subsequent abstractions. In fact, eq. (2) may be aided if the parent C_2HCl_3 is excited from a collision with an energetic free electron. Since $k_1 << k_2$, eqs. (2) and (3) can be combined to form

$$2\,H + C_2HCl_3 \xrightarrow{k_1'} HCl + C_2H_2Cl_2 \quad (5)$$

So, k_1' is on the order of k_1. A steady state analysis on H results in

$$d(H)/dt = 0 = k_o(H_2) - k_1'(H)^2(C_2HCl_3) - k_3(H)^2 \quad (6)$$

Since k_1 is slow, reaction (2) is rate limiting and

$$r_A = d(C_2HCl_3)/dt = -k_1(H)(C_2HCl_3) \quad (7)$$

From eq. (6),

$$(H)^2 = \frac{k_o\,(H_2)}{k_1'\,(C_2HCl_3) + k_3} \quad (8)$$

Assuming that $k_3 << k_1'(C_2HCl_3)$, eq. (8) reduces to

$$(H) = (k_o/k_1')^{1/2}\,(H_2)^{1/2}\,(C_2HCl_3)^{-1/2} \quad (9)$$

Substitution of eq. (9) into eq. (7) results in a rate expression with the experimentally observed orders

$$r_A = d(C_2HCl_3)/dt = -k_1(k_o/k_1')^{1/2}\,(H_2)^{1/2}\,(C_2HCl_3)^{1/2} \quad (10)$$

4. $C_2HCl_3 + H_2$ Alternate Mechanism

An alternative mechanism for the reaction $C_2HCl_3/H2$ resulting in a rate expression showing 1/2 order kinetic dependence in C_2HCl_3 is presented below. It relies on a chain reaction with an active propagating C_2Cl radical for conversion of parent C_2HCl_3.

$$e^- (KE) + C_2HCl_3 \xrightarrow{k_1} HCl + C_2Cl_2 + e^- \quad (1)$$

$$C_2Cl_2 + H \xrightarrow{k_2} HCl + C_2Cl \quad (2)$$

$$C_2Cl + C_2HCl_3 \xrightarrow{k_3} C_2ClH + C_2Cl_3 \quad (3)$$

$$C_2Cl_3 + H \xrightarrow{k_4} HCl + C_2Cl + Cl \quad (4)$$

$$C_2Cl + C_2Cl \xrightarrow{k_5} C_4Cl + Cl \quad (5)$$

$$C_2Cl_3 + C_2Cl_3 \xrightarrow{k_6} C_4Cl_5 + Cl \quad (6)$$

Reactions (1) and (2) are chain initiation and transfer steps. Reactions (3) and (4) are chain propagation steps. Reactions (5) and (6) are chain termination steps in that products continue to react forming stable end adducts. The balance equation for C_2HCl_3 is

$$d(C_2HCl_3)/dt = -k_1(C_2HCl_3) - k_3(C_2Cl)(CHCl_3) \quad (7)$$

where $k_1 = k_1'(e^-)$ and (e^-) is constant for a given power input. Steady state approximations are made for (C_2Cl), (C_2Cl_2), and (C_2Cl_3).

$$d(C_2Cl)/dt = 0 = k_2(C_2Cl_2)(H) - k_3(C_2Cl)(C_2HCl_3) + k_4(C_2Cl_3)(H) - k_5(C_2Cl)^2 \quad (8)$$

$$d(C_2Cl_2)/dt = 0 = k_1(C_2HCl_3) - k_2(C_2Cl_2)(H) \quad (9)$$

$$d(C_2Cl_3)/dt = 0 = k_3(C_2Cl)(C_2HCl_3) - k_4(C_2Cl_3)(H) - k_6(C_2Cl_3)^2 \quad (10)$$

Since (C_2HCl_3) and (H) are much greater than (C_2Cl), equation (8) reduces to

$$0 = k_2(C_2Cl_2)(H) - k_3(C_2Cl)(C_2HCl_3) + k_4(C_2Cl_3)(H) \quad (11)$$

Adding eqs. (11) and (10) results in

$$0 = k_2(C_2Cl_2)(H) - k_6(C_2Cl_3)^2 \quad (12)$$

From (9) we have

$$(C_2Cl_2) = k_1(C_2HCl_3)/k_2(H) \quad (13)$$

Substitute (13) into (12) to get

$$(C_2Cl_3) = (k_1(C_2HCl_3)/k_6)^{1/2} \qquad (14)$$

Substitute (13) and (14) into (11) to obtain

$$(C_2Cl) = k_1/k_3 + (k_4/k_3)(H)(k_1/k_6)^{1/2}(C_2HCl_3)^{-1/2} \qquad (15)$$

Assuming that the rate of propagation is much greater than the rate of initiation, $k_3 >> k_1$, eq. (15) reduces to

$$(C_2Cl) = (k_4/k_3)(H)(k_1/k_6)^{1/2}(C_2HCL_3)^{-1/2} \qquad (16)$$

Also assuming that $k_3(C_2Cl) >> k_1$ reduces eq. (7) to

$$d(C_2HCl_3)/dt = -k_3(C_2Cl)(C_2HCl_3) \qquad (17)$$

Finally, substituting (16) into (17) results in

$$d(CHCl_3)/dt = -k''(H)(C_2HCl_3)^{1/2} \qquad (18)$$

where $k'' = k_4(k_1/k_6)^{1/2}$. We can include the follwing reactions involving H_2 and H

$$e^- (KE) + H_2 \xrightarrow{k_o} H + H + e^- \qquad (19)$$

$$H + H + M \xrightarrow{k_7} H_2 + M \qquad (20)$$

A steady state balance can now be written for (H)

$$d(H)/dt = 0 = k_o(H_2) - k_2(H)(C_2Cl_2) - k_4(H)(C_2Cl_3) - k_7(H)^2 \quad (21)$$

If we assume that $k_7(H)^2$ and (H_2) are greater than the other terms in eq. (21) due to the excess of H_2, then eq. (21) results in

$$(H) = (k_o(H_2)/k_7)^{1/2} \quad (22)$$

Substitution of eq. (22) into eq. (18) finally results in a rate expression with the observed kinetic orders

$$d(C_2HCl_3)/dt = -k''_o (H_2)^{1/2}(C_2HCl_3)^{1/2} \quad (23)$$

where $k''_o = k_4(k_1k_o/k_6k_7)^{1/2}$.

5. $C_2HCl_3 + H_2O$ Mechanism

One series of reactions leading to 1/2 order dependence on C_2HCl_3 is shown below:

$$e^- (KE) + H_2O \xrightarrow{k_o} OH + H + e^- \quad (1)$$

$$OH + C_2HCl_3 \xrightarrow{k_1} C_2(OH)HCl3^= \quad (2)$$

$$OH + C_2(OH)HCl_3^= \xrightarrow{k_2} HOCl + C_2(OH)HCl_2 \quad (3)$$

$$OH + C_2(OH)HCl_3^= \longrightarrow H_2O + C_2(OH)Cl_3 \quad (3a)$$

$$C_2(OH)Cl_3^= \longrightarrow C(OH)Cl + CCl_2 \quad (3b)$$

$$C_2(OH)HCl_2 \longrightarrow C(OH)HCl + CCl \quad (3c)$$

$$OH + OH \xrightarrow{k_3} HO_2 + H \quad (4)$$

$$OH + OH \longrightarrow H_2O + O \quad (4a)$$

where $^=$ indicates a species vibrationally excited as a result of bond formation (e.g. the epoxide) or collision with an energetic species, such as an e^- (KE). The rate of initial addition of OH to the double bond of C_2HCl_3 is probably slower than subsequent attacks by OH on the intermediate epoxide. We can assume $k_1 << k_2$ and equations (2) and (3) can be combined to form

$$2\ OH + C_2HCl_3 \xrightarrow{k_1'} \text{Intermediates} \quad (5)$$

where the intermediates lead to stable CO and HCl formation. The constant k_1' is on the order of k_1. A steady state analysis on OH results in

$$d(OH)/dt = 0 = k_o(H_2O) - k_1'(OH)^2(C_2HCl_3) - k_3(OH)^2 \quad (6)$$

Since k_1 is slow, reaction (2) is rate limiting and

$$r_A = d(C_2HCl_3)/dt = -k_1(OH)(C_2HCl_3) \quad (7)$$

From eq. (6),

$$(OH)^2 = \frac{k_o\,(H_2O)}{k_1'\,(C_2HCl_3) + k_3} \quad (8)$$

Assuming that $k_3 << k_1'(C_2HCl_3)$, eq. (8) reduces to

$$(OH) = (k_o/k_1')^{1/2}\,(H_2O)^{1/2}\,(C_2HCl_3)^{-1/2} \quad (9)$$

Substitution of eq. (9) into eq. (7) results in a rate expression with the experimentally observed orders

$$r_A = d(C_2HCl_3)/dt = -k_1(k_o/k_1')^{1/2}\,(H_2O)^{1/2}\,(C_2HCl_3)^{1/2} \quad (10)$$

6. Calculation of Initial Chlorocarbon Concentration C_{Ao} and Feed Rate F_{Ao}

(Liquid Chlorocarbon Impinger and H_2)

For the system of $CHCl_3$ + H_2 where H_2 is bubbled through liquid $CHCl_3$ impingers, the volumetric feed rate of $CHCl_3$ is calculated as follows:

$$CHCl_3 \text{ Flow} = (\text{Total Flow})\ (P_s / P_b) \qquad (1)$$

where Total Flow = volumetric rate of $CHCl_3$ + H_2, P_s = vapor pressure of $CHCl_3$ at the temperature of the impingers, and P_b = total pressure in the impingers. Assuming P_b = 760 mm Hg and P_s = 163 mm Hg (at 21 °C), eq. (1) becomes

$$CHCl_3 \text{ Flow} = (H_2 \text{ Flow} + CHCl_3 \text{ Flow})\ (163/760) \qquad (2)$$

Solving for $CHCl_3$ Flow,

$$CHCl_3 \text{ Flow} = \frac{(163/760)}{\{1 - (163/760\}}\ (H_2 \text{ Flow}) \qquad (3)$$

$$CHCl_3 \text{ Flow} = (0.273)\ (H_2 \text{ Flow}) \qquad (3a)$$

where $CHCl_3$ Flow and H_2 Flow are respective volumetric flow rates of $CHCl_3$ and H_2 in similar units. The H_2 Flow (in STD

cm^3/min) is known from a calibrated flowmeter upstream of the impingers.

The mole fraction of $CHCl_3$ in the feed is determined by

$$\text{Mol Frac} = \frac{(0.273)\ (H_2\ \text{Flow})}{(0.273)(H_2\ \text{Flow}) + (H_2\ \text{Flow}) + H_2\ (\text{suppl})} \qquad (4)$$

where H_2 (suppl) is the volumetric flow of any supplemental H_2 which is fed in separately, bypassing the impingers. Equation (4) assumes that there are no other species in the feed.

Initial $CHCl_3$ concentration C_{Ao} is now calculated by

$$C_{Ao} = \frac{(\text{Mol Frac})\ (P_r)}{(R)\ (T)} \qquad (5)$$

where Mol Frac = mole fraction of $CHCl_3$ calculated from eq. (4), P_r = pressure of the plasma reactor flow tube with the plasma on, R = gas constant, and T = temperature of the feed (room temperature for the present setup). For example, at room temperature = 294 K, plasma reactor pressure = 2.0 mmHg, and Mol Frac of $CHCl_3$ = 0.1, calculate

$$C_{Ao} = (0.1)\ (2/760)\ (1/0.0821)\ (1/294)$$

$$C_{Ao} = 10.9 \text{ micro moles / liter} \qquad (6)$$

The initial molar flow rate of $CHCl_3$ is calculated by

$$F_{Ao} = \frac{(P_b)\ (CHCl_3\ Flow)}{(R)\ (T)} \qquad (7)$$

For example, at P_b = 1 atm, $CHCl_3$ Flow = 5 STD cm^3/min, and T = 294 K, calculate

$$F_{Ao} = (1)\ (5)\ (1/0.0821)\ (1/294)\ (1/1000)$$

$$F_{Ao} = 207.\ \text{micro moles / minute} \qquad (8)$$

(Heated Vapor Generator)

The molar feed rate of reactant vapor drawn from a heated reservoir, as described in the Experimental Apparatus section, is calculated by

$$F_{Ao} = \frac{(P_f)\ (V_k)}{(t_f)\ (R)\ (T)} \qquad (9)$$

where P_f = pressure to which known volume is filled, V_k = known offline volume, and t_f = time to fill known volume. These measurements are taken when the vapor drawn from the

generator is directed offline and into the device pictured in Figure (3). A known volume is filled to a measured pressure in a measured time. For example, with P_f = 10 mm Hg, V_k = 2200 cm^3, t_f = 0.9 minutes, and T = 294 k (room temperature), the molar flow rate is

$$F_{Ao} = (10/760)\ (2200/1000)\ (1/0.0821)\ (1/294)\ (1/0.9)$$

$$F_{Ao} = 1333.\ \text{micro moles / minute} \qquad (10)$$

Mole fractions are calculated as in eq. (4) with consistent units. Concentrations are calculated as in eq. (5).

7a. Data for Kinetic Analyses

$(CHCl_3 + H_2)$

M	$F_{Ao}*10^6$ (mol/min)	$C_{Ao}*10^6$ (mol/lit)	X_A	P (mmHg)	$\frac{C_{Ao}\ M^{.5}*10}{F_{Ao}}$ (min/lit)	$\frac{(1+.1X_A)\ dX_A}{(1-X_A)^{.5}(1-X_A/(3M))^{.5}}$
78.4	96.4	1.68	0.837	2.48	1.543	1.251
64.8	118.0	2.08	0.807	2.55	1.419	1.174
48.0	162.0	2.88	0.777	2.62	1.232	1.103
37.5	213.0	3.75	0.780	2.68	1.078	1.111
29.9	274.0	4.79	0.676	2.75	0.956	0.895
21.8	396.0	6.78	0.669	2.88	0.799	0.883
19.2	462.0	8.00	0.650	3.01	0.759	0.848
16.3	568.0	9.75	0.541	3.14	0.693	0.666
13.3	234.0	7.78	0.780	2.06	1.213	1.115
13.3	325.0	10.6	0.820	2.81	1.189	1.212
13.3	436.0	14.4	0.726	3.78	1.200	0.996

$(C_2HCl_3 + H_2O)$

M	$F_{Ao}*10^6$ (mol/min)	$C_{Ao}*10^6$ (mol/lit)	X_A	P (mmHg)	$\frac{C_{Ao}\ M^{.5}*100}{F_{Ao}}$ (min/lit)	$\frac{(1+.9X_A)\ dX_A}{(1-X_A)^{.5}(1-X_A/(1.5M))^{.5}}$
1.55	1087.	39.96	0.969	1.897	4.583	3.007
2.19	1921.	36.38	0.914	2.158	2.802	2.324
1.91	2198.	44.67	0.780	2.420	2.812	1.623
1.41	2991.	55.54	0.504	2.485	2.202	0.790
1.72	2449.	46.59	0.595	2.354	2.493	1.007
3.03	1155.	29.66	0.949	2.224	4.471	2.532
2.29	1155.	33.15	0.889	2.027	4.341	2.144
0.59	1595.	46.42	0.593	1.373	2.237	1.230
3.38	1431.	30.55	0.984	2.485	3.922	2.926
1.50	682.0	29.50	0.937	1.373	5.303	2.662
0.53	1603.	50.51	0.558	1.439	2.298	1.142
0.77	1603.	53.49	0.603	1.757	2.922	1.162
1.60	1417.	37.83	0.602	1.831	3.380	1.033
1.96	1326.	36.85	0.700	2.027	3.889	1.316
2.68	1312.	32.52	0.643	2.224	4.056	1.111
6.16	948.0	20.63	0.933	2.747	5.402	2.304
2.38	560.0	22.91	0.999	1.439	8.449	3.416
1.04	1279.	43.07	0.734	1.635	3.436	1.577
0.80	1910.	52.69	0.702	1.766	2.472	1.545
1.02	1201.	40.04	0.645	1.504	3.367	1.234
1.28	959.0	33.98	0.771	1.439	4.004	1.676
2.01	610.0	24.55	0.830	1.373	5.703	1.844
1.51	819.0	30.89	0.767	1.439	4.627	1.615
4.92	343.0	13.06	0.999	1.439	6.310	3.643

$(C_2HCl_3 + H_2)$

M	$F_{Ao}*10^6$ (mol/min)	$C_{Ao}*10^6$ (mol/lit)	X_A	P (mmHg)	$\frac{C_{Ao}\ M^{.5}*10}{F_{Ao}}$ (min/lit)	$\frac{(1+.05X_A)\ dX_A}{(1-X_A)^{.5}(1-X_A/(2M))^{.5}}$
50.7	133.8	2.01	0.912	1.929	1.068	1.447
39.3	184.5	2.70	0.870	2.027	0.923	1.313
36.1	206.8	3.03	0.828	2.093	0.882	1.203
32.6	237.2	3.56	0.814	2.224	0.858	1.166
29.0	279.7	4.21	0.812	2.354	0.810	1.161

7b. Cumulative Product Distributions

$(CHCl_3 + H_2)$

Molar Feed Carbon Disposition (%)

C_2HCl_3 Conver.	C_2 to C_4 Hydrocarbons	C_6 Hydrocarbons	Non-Parent Chlorocarbons	CH_4 + $C_{(s)}$	Unconv. C_2HCl_3
53.0	37.4	0.9	2.6	13.8	47.0
67.0	30.9	1.1	2.0	32.6	33.0
80.7	25.4	0.9	7.8	46.4	19.3
83.7	27.2	2.4	4.9	49.2	16.3

$(C_6H_5Cl + H_2)$

Molar Feed Carbon Disposition (%)

C_6H_5Cl Conc.*	C_2 to C5 Hydrocarbons	C_6 to C_7 Hydrocarbons	Non-Parent Chlorocarbons	CH_4 + $C_{(s)}$	Unconv. C_6H_5Cl
0.42	36.4	4.9	0.0	57.8	0.7
0.53	33.5	4.4	0.0	60.9	1.3
0.58	30.0	4.3	0.0	65.1	0.6
0.63	27.5	3.9	0.0	67.8	0.7
0.74	26.8	4.9	0.0	66.8	1.3

$(C_2HCl_3 + H_2)$

Molar Feed Carbon Disposition (%)

C_2HCl_3 Conver.	C_2 to C_4 Hydrocarbons	C_6 to C_7 Hydrocarbons	Non-Parent Chlorocarbons	Graphitic $C_{(s)}$	Unconv. C_2HCl_3
81.2	42.2	4.2	12.5	22.1	18.8
81.4	37.3	2.7	12.8	28.5	18.6
82.8	38.7	4.8	12.0	27.3	17.1
87.0	35.6	3.7	10.0	37.4	13.0
91.2	43.5	3.6	9.0	35.1	8.8

$(C_2HCl_3 + H_2O)$

Molar Feed Carbon Disposition (%)

C_2HCl_3 Conver.	C_2 to C3 Hydrocarbons	C_6 to C_7 Hydrocarbons	Non-Parent Chlorocarbons	CO + $C_{(s)}$	Unconv. C_2HCl_3
50.4	11.8	0.0	26.4	12.3	49.6
60.2	11.0	0.0	22.8	26.4	39.8
70.0	9.8	0.0	10.5	49.8	30.0
78.1	10.0	0.0	10.4	57.6	21.9
96.9	7.6	0.0	4.4	84.9	3.1

($C_2HCl_3 + H_2$)

Molar Feed Chlorine Disposition (%)

C_2HCl_3 Conversion	Non-Parent Chlorocarbons	HCl	Unconverted C_2HCl_3
81.2	8.7	72.5	18.8
81.4	8.2	73.2	18.6
82.8	9.6	73.2	17.2
87.0	8.9	78.2	13.0
91.2	7.2	84.0	8.8

($C_2HCl_3 + H_2O$)

Molar Feed Chlorine Disposition (%)

C_2HCl_3 Conversion	Non-Parent Chlorocarbons	HCl	Unconverted C_2HCl_3
50.0	17.1	33.3	50.0
60.0	11.8	48.4	40.0
70.0	6.0	64.0	30.0
78.0	6.6	71.4	22.0
97.0	3.5	93.3	3.0

($CHCl_3 + H_2$)

Molar Feed Chlorine Disposition (%)

$CHCl_3$ Conversion	Non-Parent Chlorocarbons	HCl	Unconverted $CHCl_3$
53.0	0.4	54.0	47.0
67.0	0.5	66.0	33.0
80.0	1.8	79.0	19.3
83.0	2.0	82.0	16.0

7c. Data for Arrhenius-type Experiment

Data for Arrhenius-Type Experiment

Input Volts	Input Amps	Input kWatts	$\frac{1}{kWatts}$	$CHCl_3$ Conversion	k (sec^{-1})	ln k
85	2.5	0.21	4.7	66.9	3.9	1.36
90	3.6	0.32	3.1	77.4	4.8	1.58
95	5.2	0.50	2.0	87.1	6.0	1.79
105	7.4	0.77	1.3	93.7	7.0	1.95
110	7.5	0.82	1.2	94.9	7.3	1.98

REFERENCES

1. L. Manson and S. Ungett, "Hazardous Material Incinerator Design Criterion," U.S. EPA 600/2.79.198 NTIS No. PB80-131964 (1979).

2. H. Faber, "New York Times," p. 50, Nov. 8 (1981).

3. J. L. Roberts, Jr. and D.T. Sawyer, Journal of the American Chemical Society, 103, 712 (1981).

4. L. Pytlewski, et. al., "Reactions of PCB's with Na, O_2, and Polyethylene Glycols, U.S. EPA 600/90.80.011 NTIS No. PB80-175094 (1980).

5. C. Botre, et. al., Environmental Science and Technology, 13(2): 228-231 (1979).

6. B. C. Hertzler, et. al., "Development of Microwave Plasma Detoxification Process for Hazardous Wastes (Phase III)," U.S. EPA Contract 68-03-2190, Dec. 1979.

7. a. Zimpro, Inc., Rothchild, Wisconsin, Chemical Engineering Progress, 8: 46 (1979).
   b. R. A. Miller and M. D. Swientoniewski, "The Destruction of Various Organic Substances by a Catalyzed Wet Oxidation Process," IT Enviroscience, Knoxville, Tenn.

8. M. Modell, U. S. Patent 4,338,199, July 6 (1982).

9. S. J. Arnold, et. al., Canadian Journal of Chemistry, 52, 271 (1974).

10. W.A. Rubey, et. al., "Thermal Decomposition Properties of Toxic Organic Substances," APCA Conference of Hazardous Waste Incineration - Proceedings, Apr. 30, 1982, Newark, N.J.

11. W. A. Rubey and D. S. Duvall, "Laboratory Evaluation of High Temperature Destruction of PCB's and Related Compounds," U.S. EPA 600/6.77, 228 (1977).

12. S. Chari, Master's Thesis, Dept. of Chemical Engineering and Chemistry, New Jersey Institute of Technology (1981).

13. A. Westenberg and N. DeHaas, Journal of Chemical Physics, 67, 2388 (1977).

14. M. Costes, et. al., Chemical Physics Letters, 61, 588 (1979).

15. S. C. Chuang, Master's Thesis, Dept. of Chemical Engineering and Chemistry, New Jersey Institute of Technology (1982).

16. S. C. Chuang, Master's Thesis, Dept. of Chemical Engineering and Chemistry, New Jersey Institute of Technology (1982).

17. J. R. Hollahan and A.T. Bell (eds.), Techniques and Applications of Plasma Chemistry, J. Wiley & Sons, New York (1974).

18. L. C. Brown and A. T. Bell, Industrial and Engineering Chemistry Fundamentals, 13, 3 (1974).

19. L. J. Bailin, et. al., Environmental Science and Technology, 12, 673 (1978).

20. L. M. Faires, American Laboratory, Nov. (1982).

21. S. J. Arnold, et. al., Canadian Journal of Chemistry, 53, 2419 (1975).

22. A. Westenberg and N. DeHaas, Journal of Chemical Physics, 62, 3321 (1975).

23. a. F. C. Fehsenfeld, et. al., Review of Scientific Instruments, 36, 294 (1965)
b. A. T. Bell, Industrial and Engineering Chemistry Fundamentals, 11, 209 (1972).

24. F. E. Lichte and R. K. Skogerboe, Analytical Chemistry, 45, 399 (1973).

25. A. J. Mendelsohn, et. al., Applied Physics Letters, 38, 603 (1981).

26. R. A. Gottscho, et. al., Journal of Applied Physics, 53(8) 5908 (1982).

27. R. F. Baddour and R.S. Timmins (eds.), The Application of Plasmas to Chemical Processing, MIT Press, Cambridge, Mass. (1967).

28. R. C. Weast (ed.-in-chief), Handbook of Physics and Chemistry, 47th edition, F-130, Chemical Rubber Company (1966-67).

29. R. B. Barat and J. W. Bozzelli, Review of Scientific Instruments, 52(4), 612 (1981).

30. Personal communication with Dr. B. C. Hertzler, Lockheed Palo Alto Research Laboratory, Palo Alto, Calif., 94304.

31. W. C. Gardiner, Jr., Scientific American, 2, 110 (1982).

32. R. V. Poirier and R. W. Carr, Jr., Journal of Physical Chemistry, 75(10), 1593 (1971).

33. Elemental analysis done by Galbrath Labs, Knoxville, Tenn.